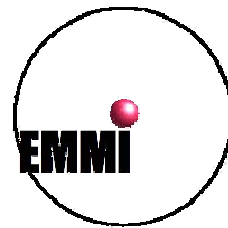


Structure and Dynamics of Highly-charged Ions: Physics at Extreme Fields

Alexandre Gumberidze

Extre**M**e **M**atter **I**nstitute, **EMMI**

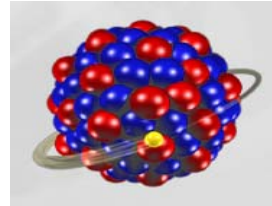


Atomic Physics at Extreme Fields with Highly Charged Heavy Ions

Scaling factors:

from H to U⁹¹⁺

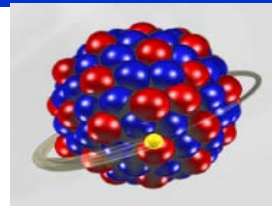
• level energy	$E_n \approx Z^2$	10^4
• hyperfine splitting	$\sim Z^3$	10^6
• nuclear size effects	$\sim Z^6$	10^{12}
• QED contributions	$\sim Z^4$	10^8



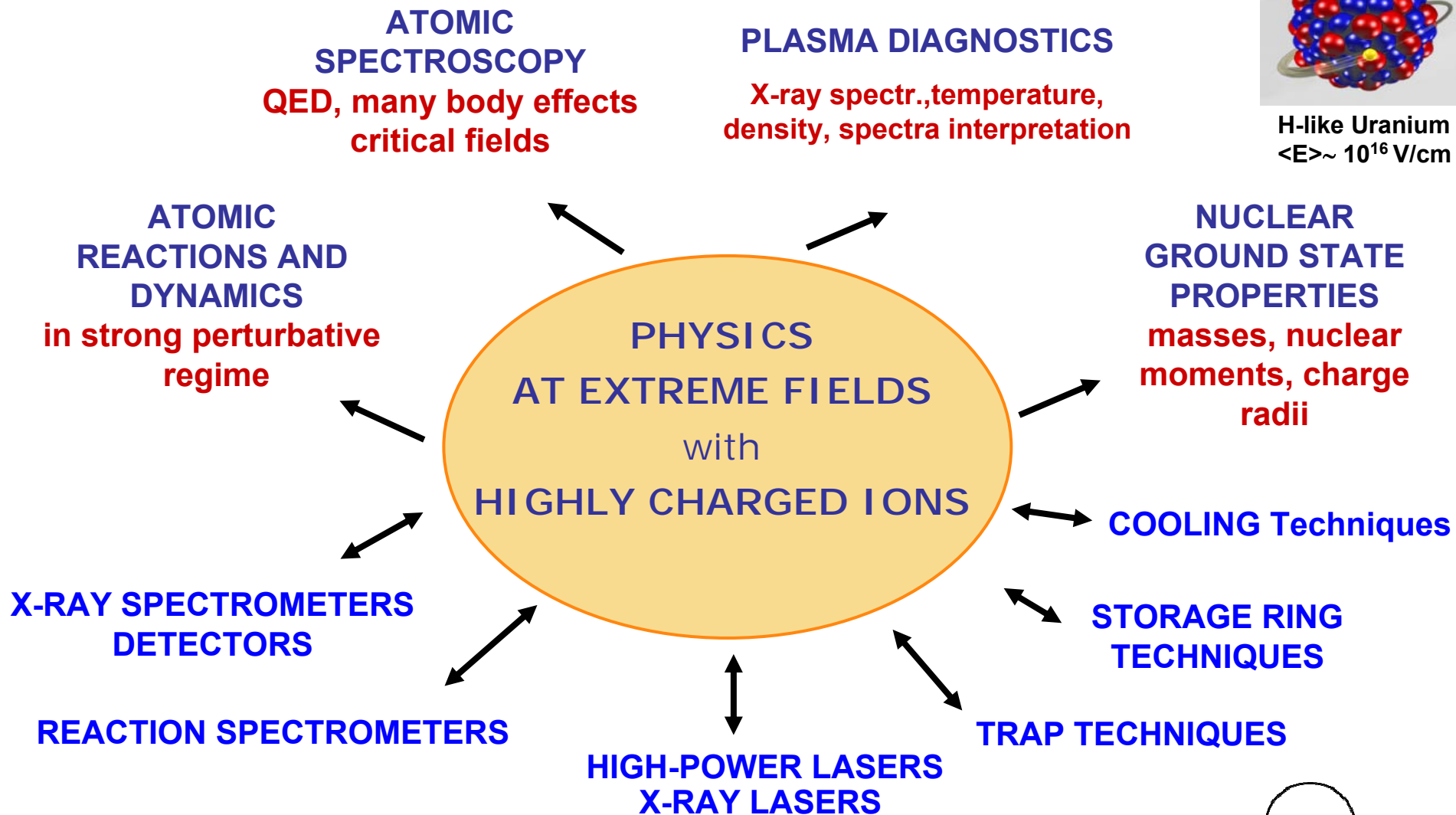
H-like Uranium
 $\langle E \rangle \sim 10^{16}$ V/cm

- Fundamental phenomena:
 - become accessible in some cases due to:
 - simpler electronic structure
 - scaling of effects with high powers of Z (QED, nuclear size,...)
- Laboratory and astrophysical plasmas:
Almost all luminous matter is ionized
- X-ray standards, fundamental constants
- Sensitivity to nuclear parameters

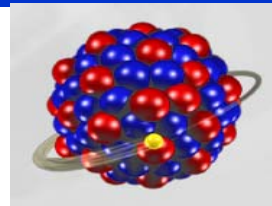
Physics at Extreme Fields with Highly Charged Heavy Ions



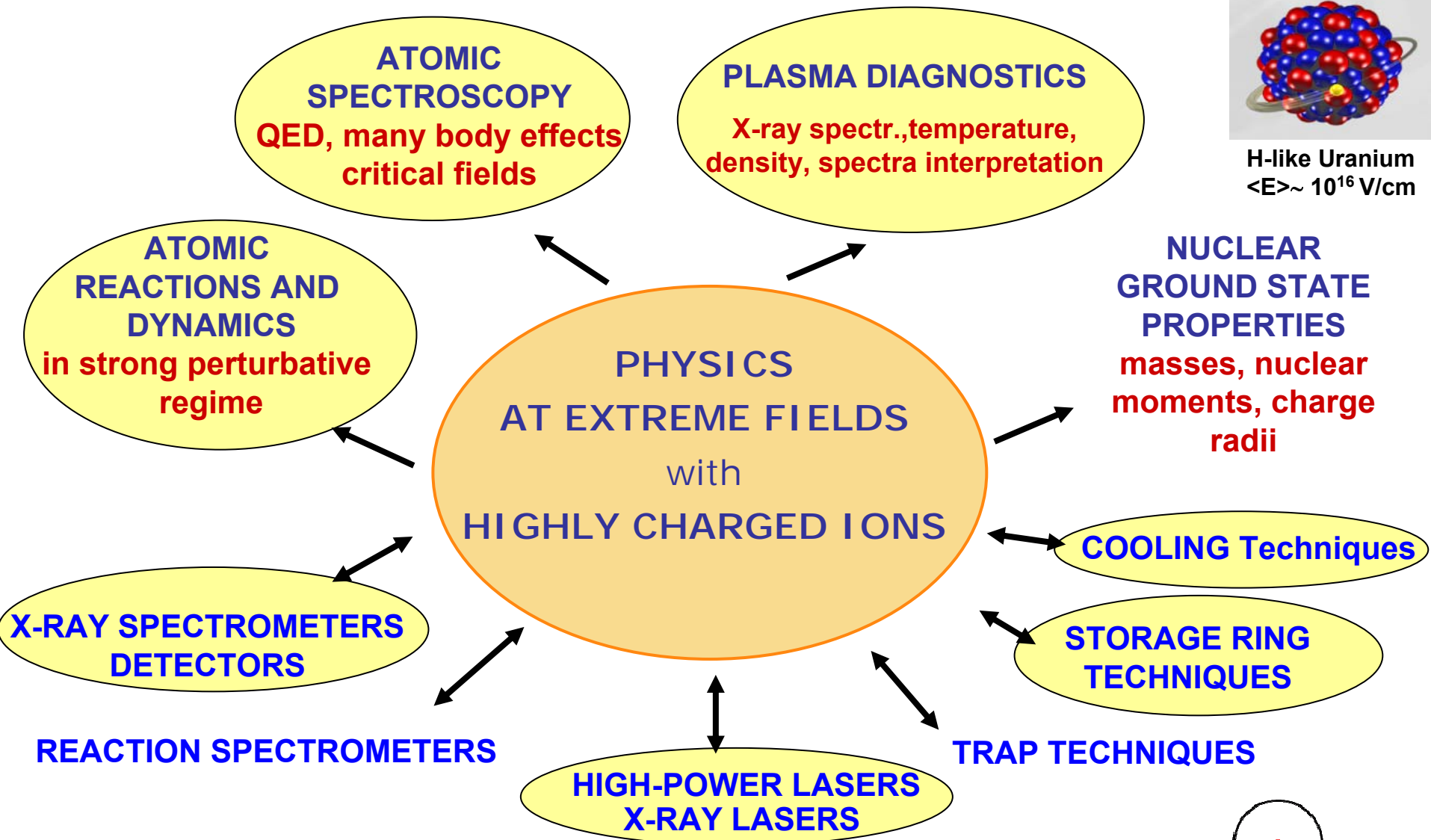
H-like Uranium
 $\langle E \rangle \sim 10^{16}$ V/cm



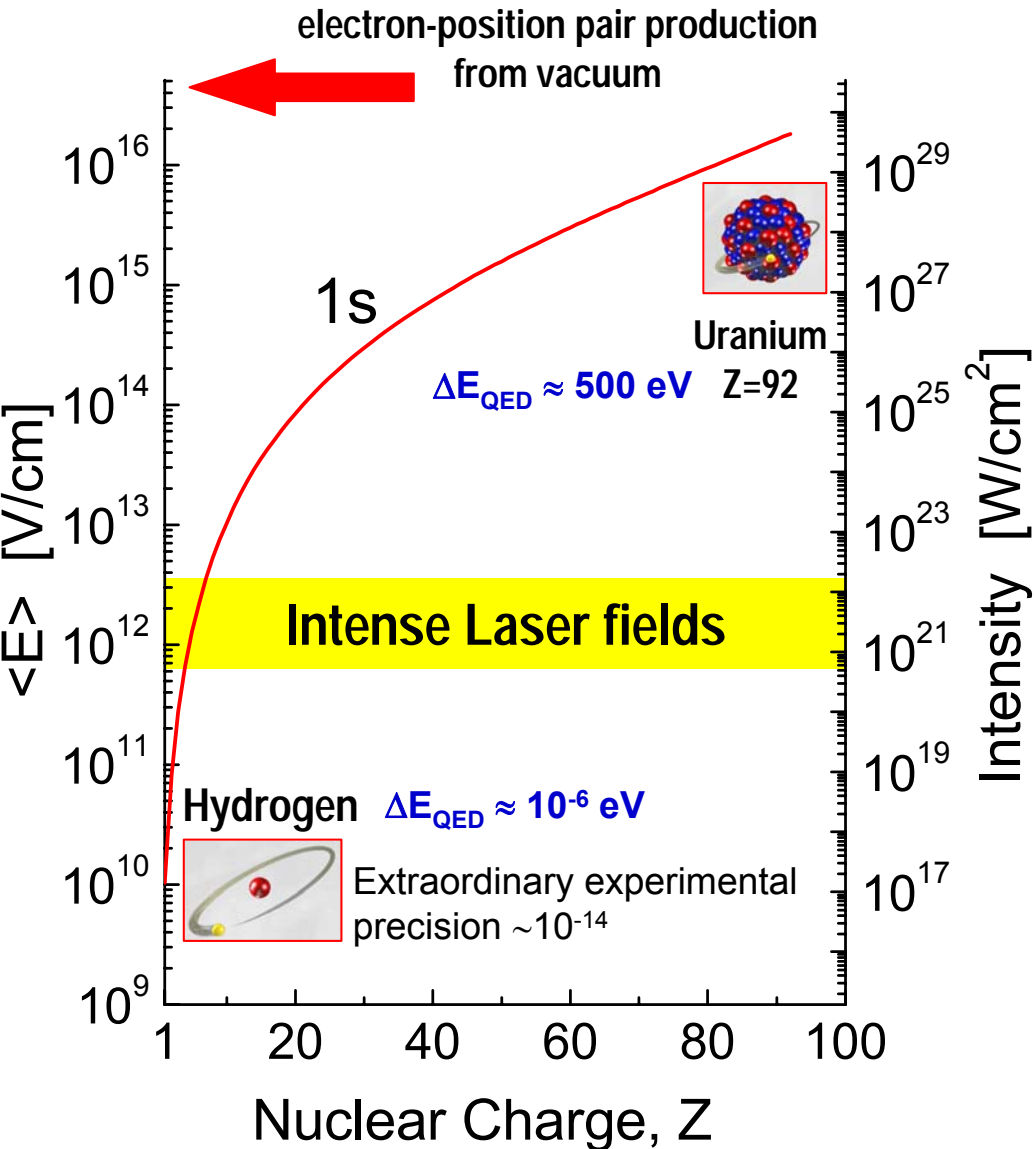
Physics at Extreme Fields with Highly Charged Heavy Ions



H-like Uranium
 $\langle E \rangle \sim 10^{16}$ V/cm



Physics in Extremely Strong Fields



Atomic Structure at High-Z

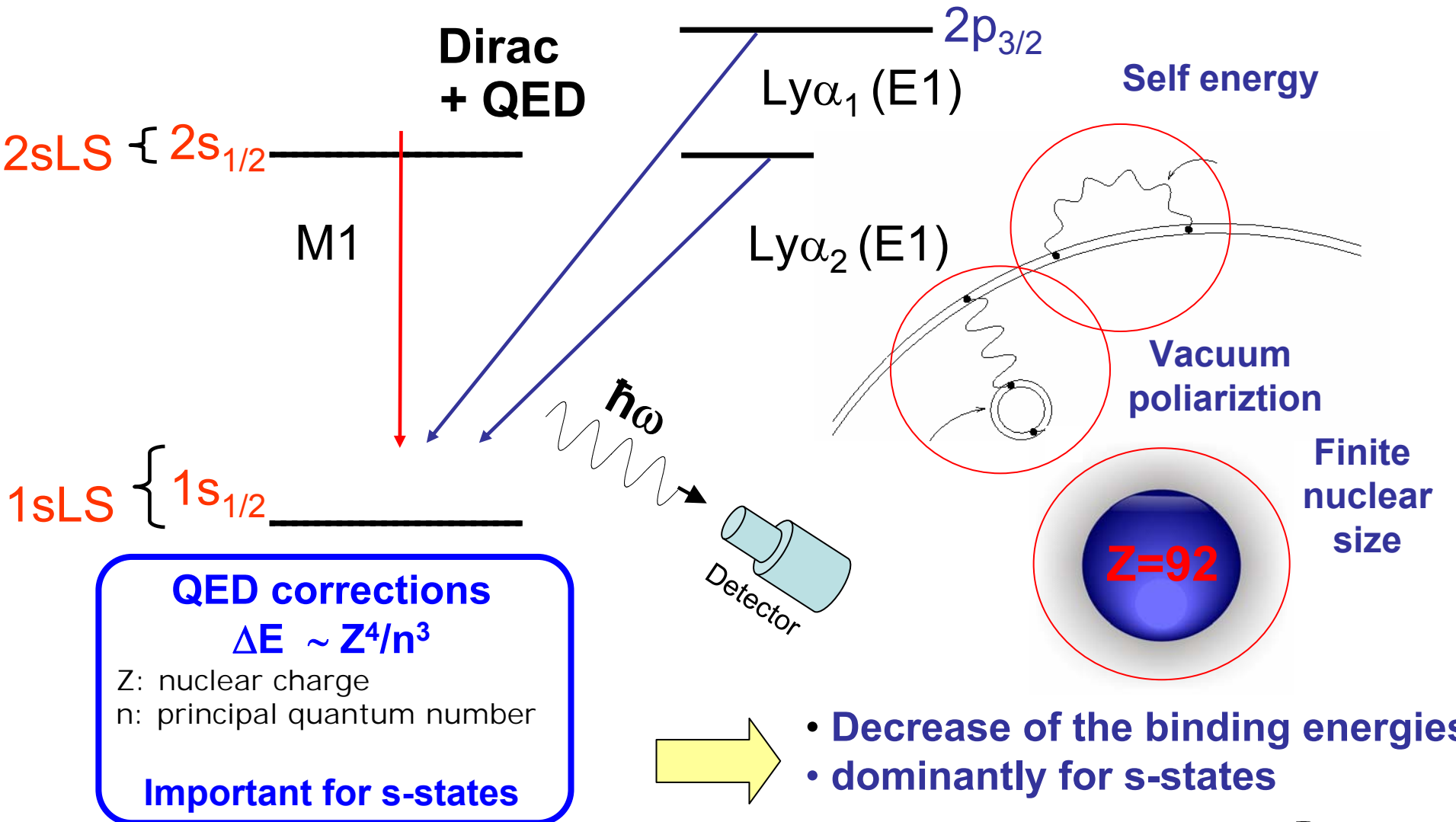
- Bound state quantum electrodynamics (QED) in extreme fields
- Effects of relativity on the atomic structure
- Electron correlation in the presence of strong fields

Atomic Collision at High-Z

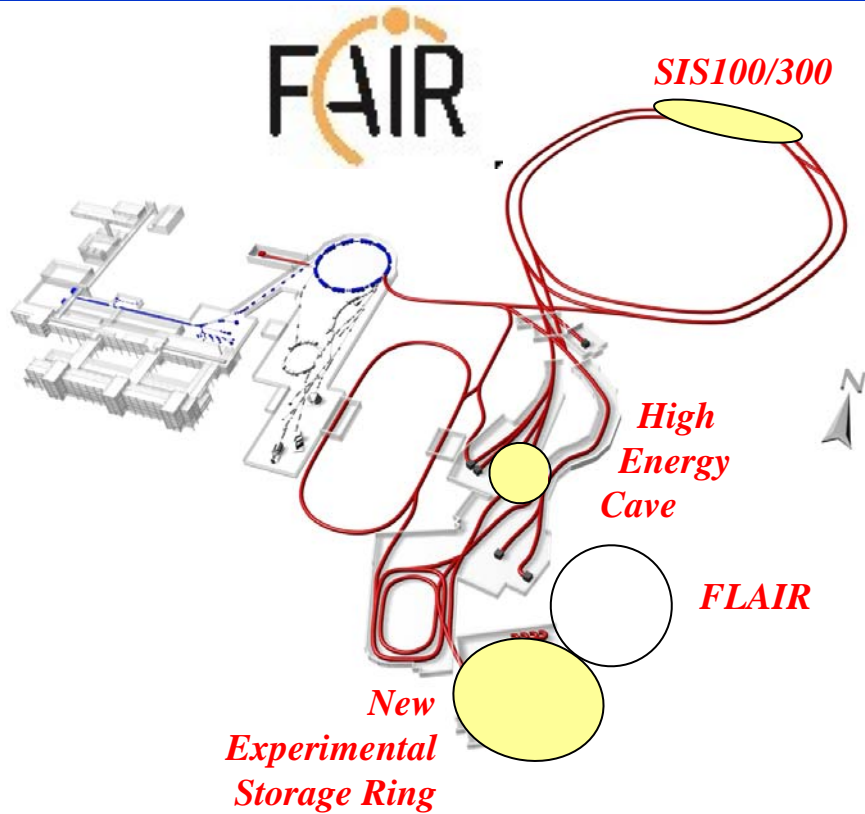
- Correlated many-body dynamics
- Photon matter interaction: e.g., photon polarization effects
- Dynamically induced strong field effects



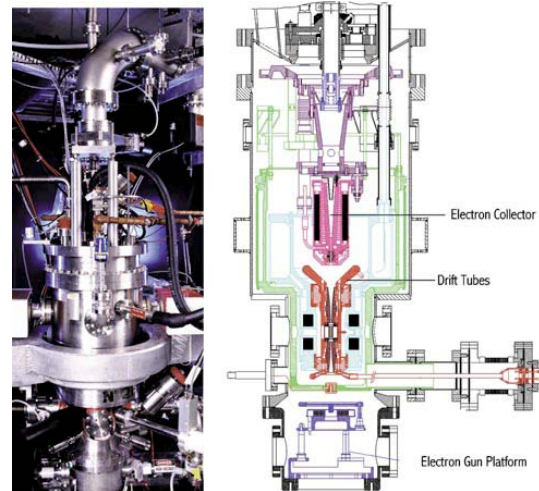
Atomic Structure of One-electron System



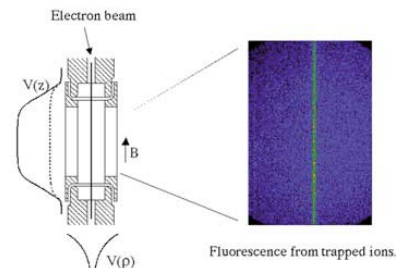
How to make HCI ?



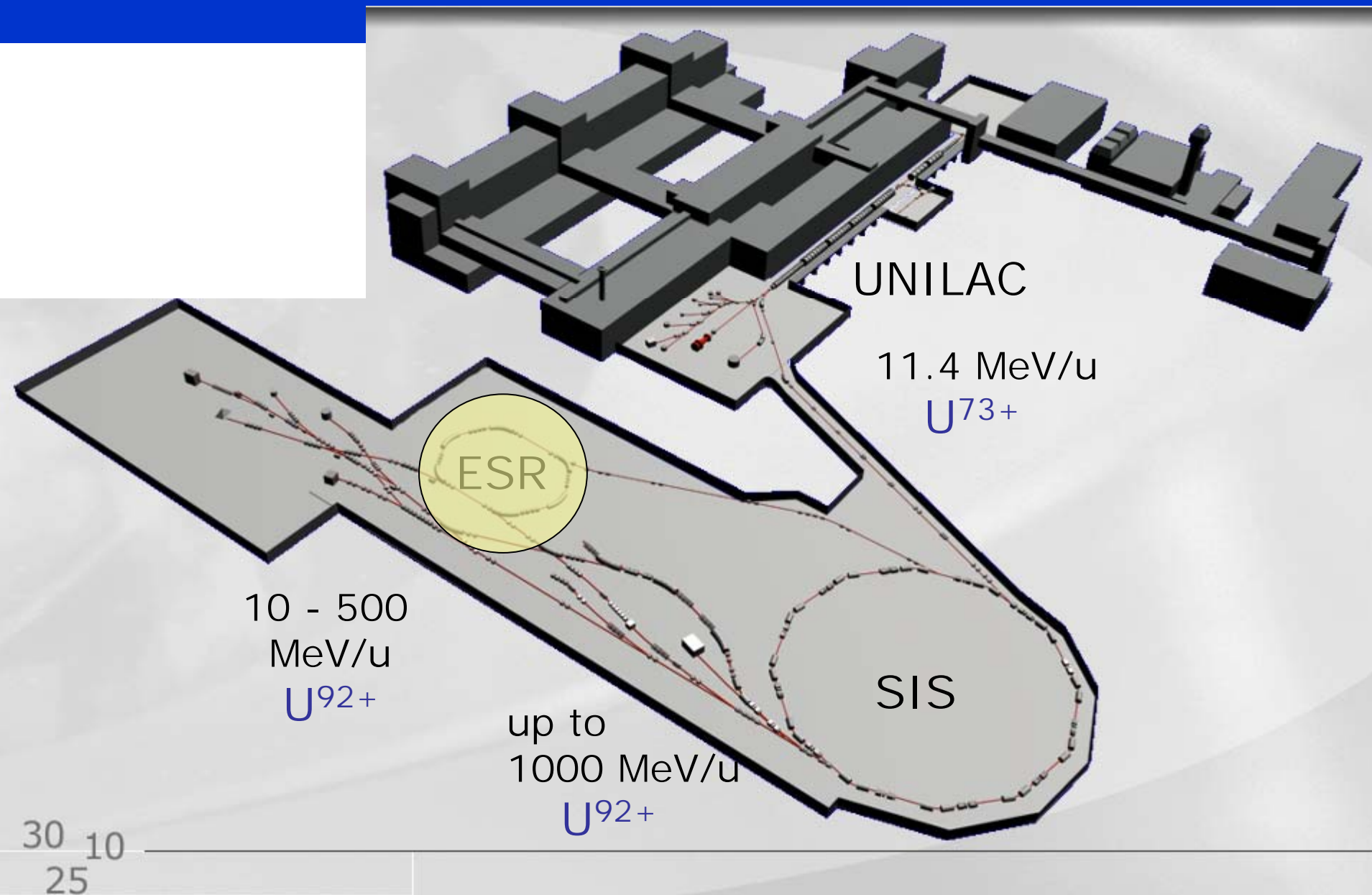
ECRIS



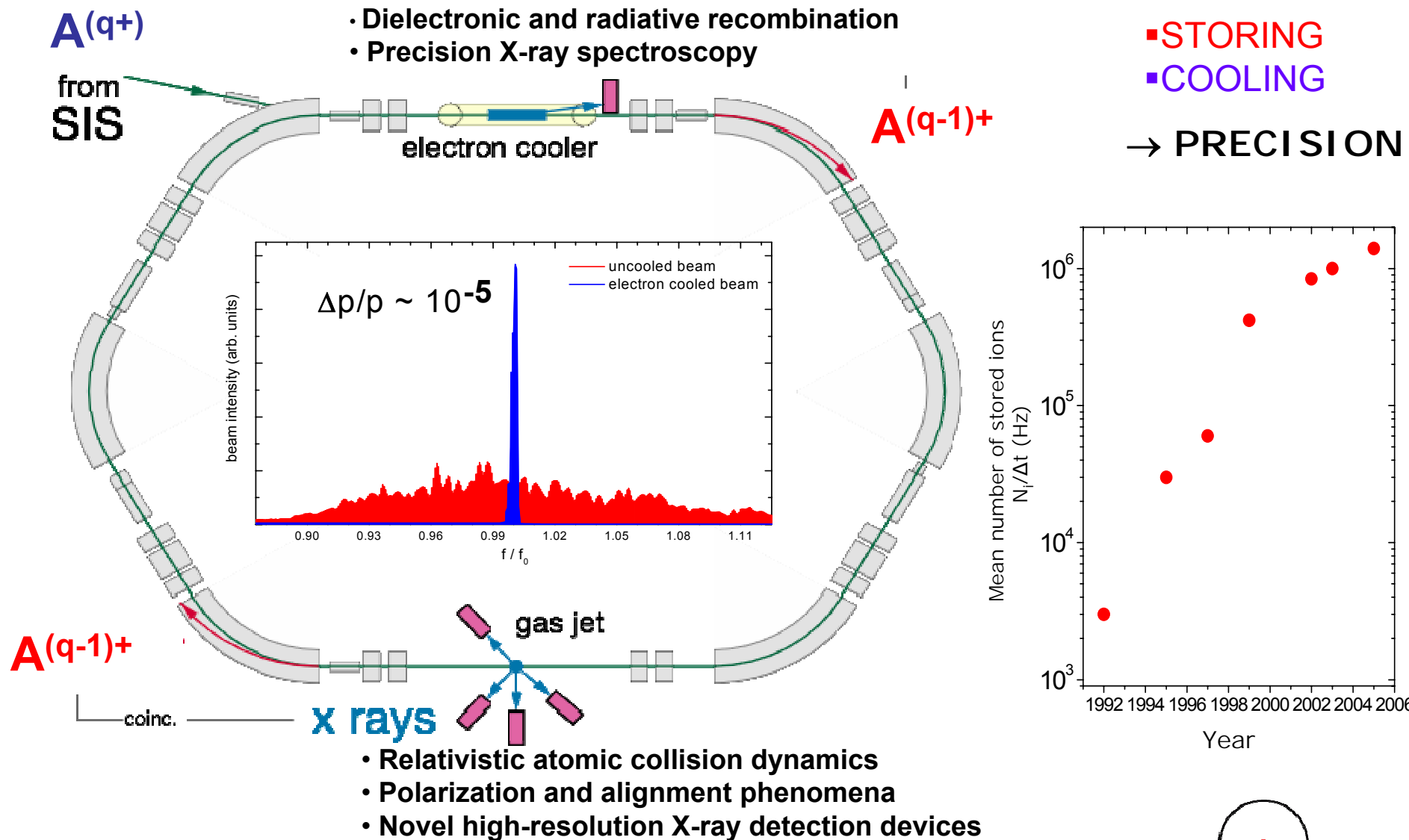
EBIT



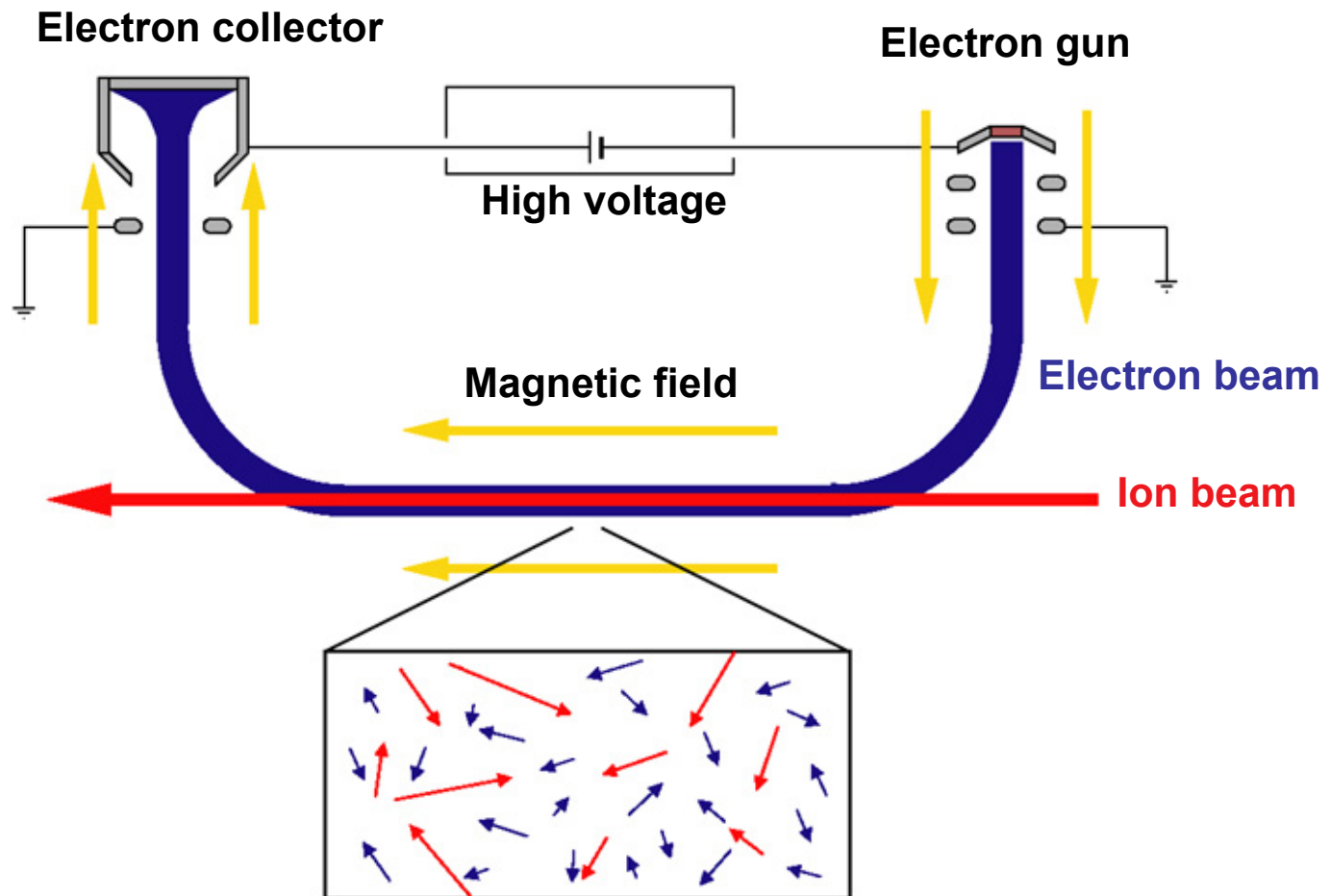
HCI Production at GSI-ACCELERATOR FACILITY



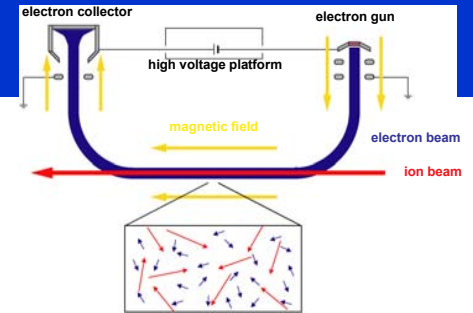
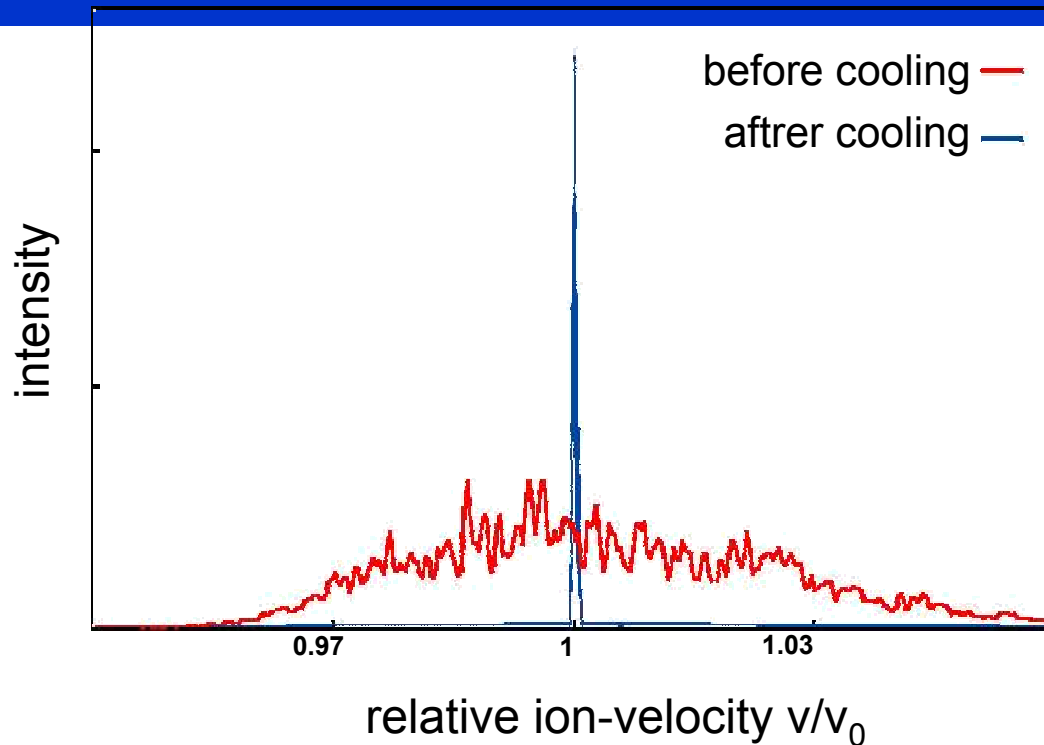
ATOMIC PHYSICS WITH STORED HIGHLY-CHARGED IONS AT THE ESR



The electron cooler



Cooled heavy-ion beams



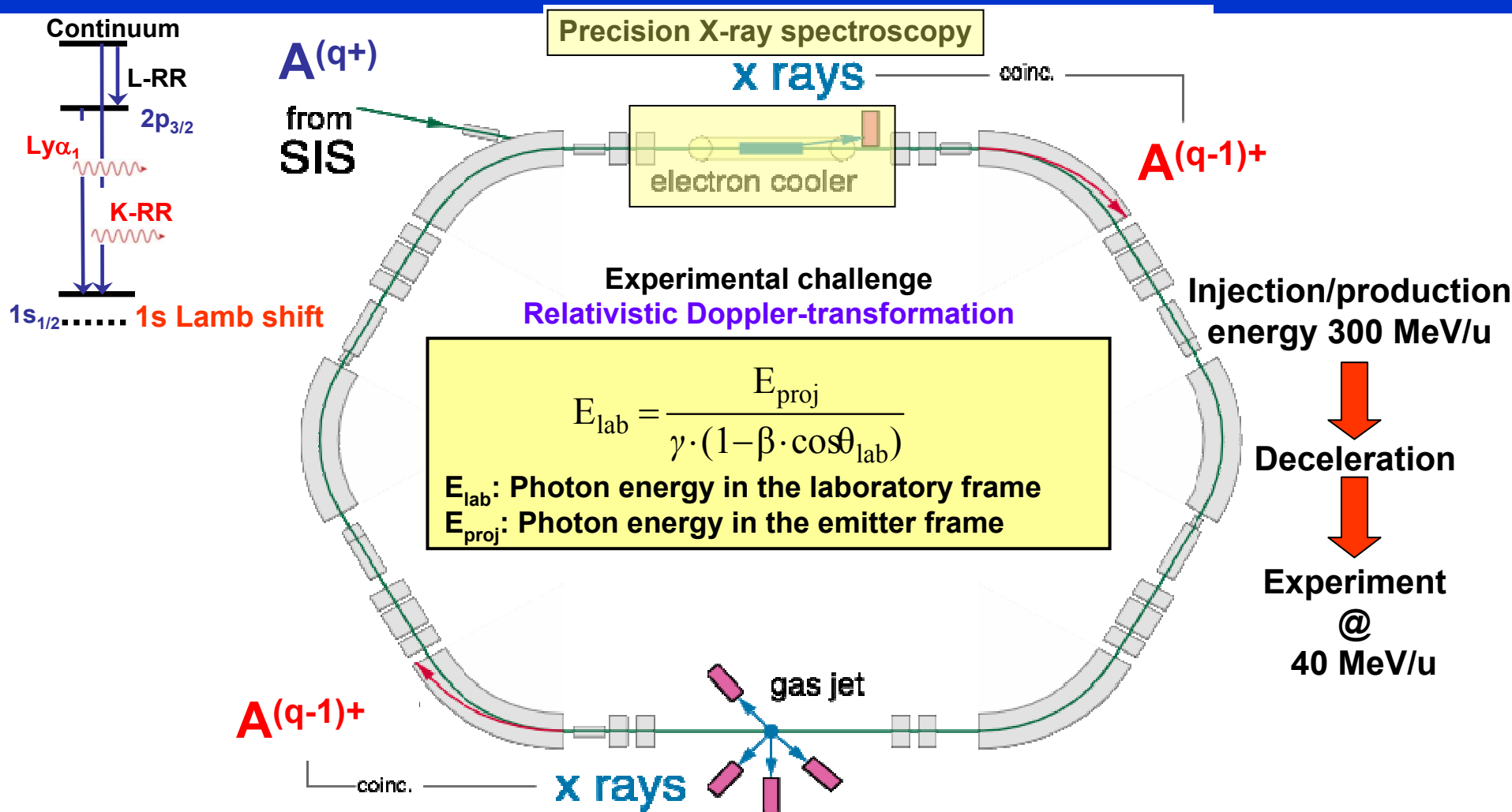
ions interact 10^6 1/s with the collinear cold electron beam

properties of cold ion beams

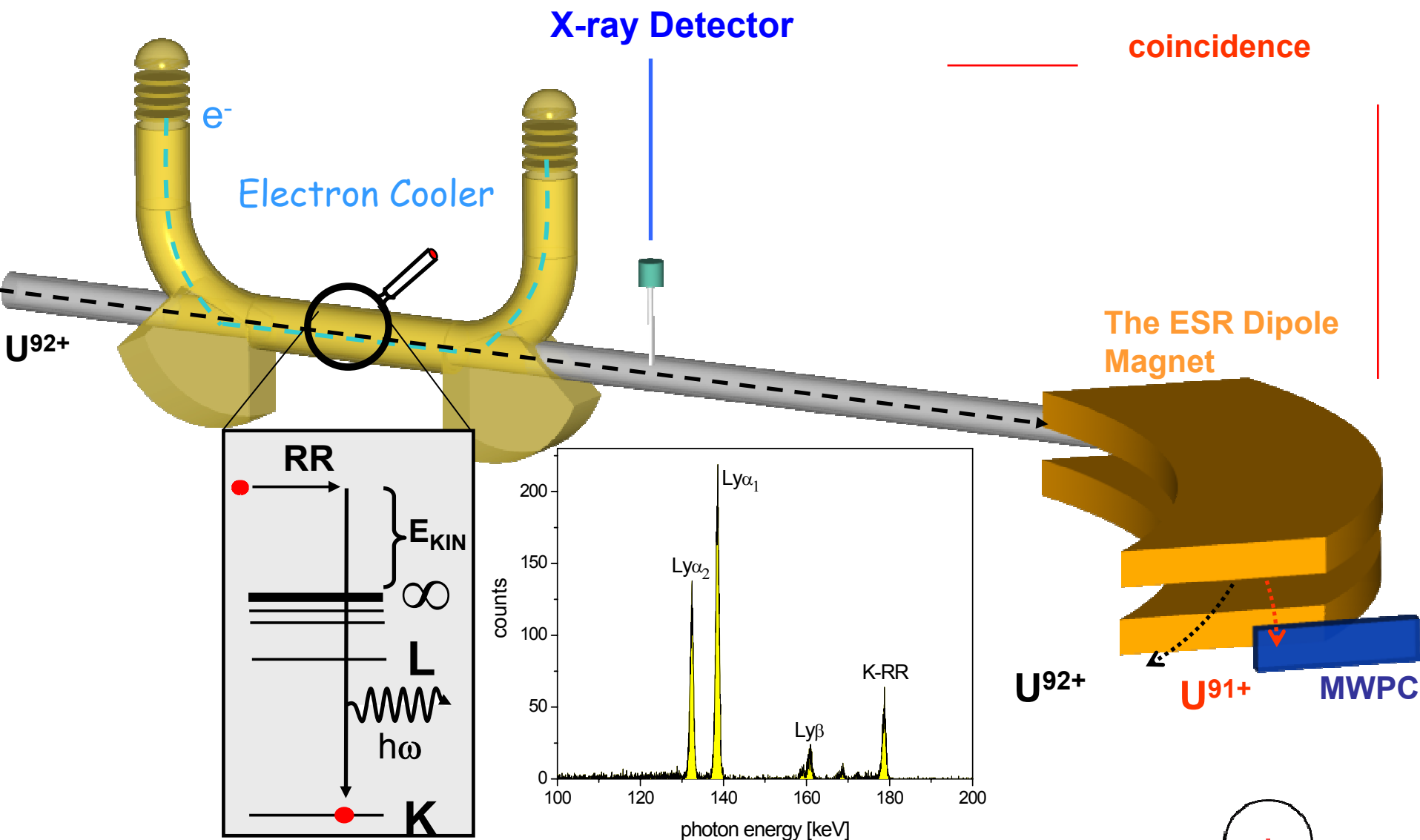
momentum width $\Delta p/p : 10^{-4} - 10^{-5}$
size 2 mm



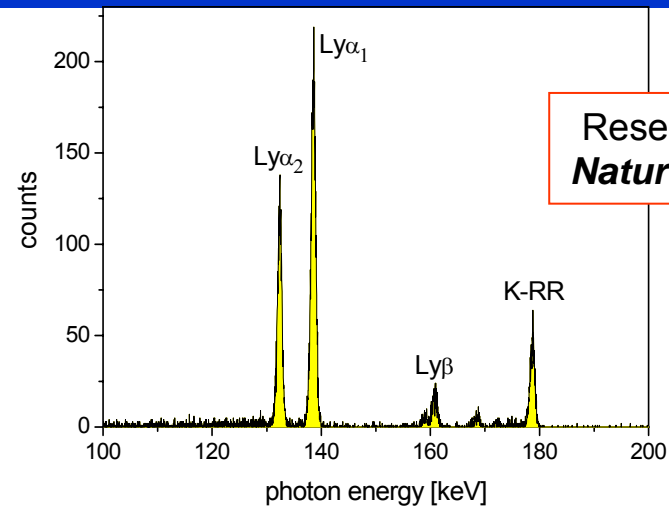
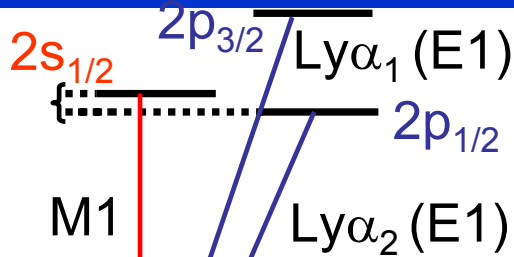
PRECISION TESTS OF BOUND-STATE QED IN EXTREME FIELDS: Lamb shift in H-like uranium



PRECISION TESTS OF BOUND-STATE QED IN EXTREME FIELDS: The Two-electron Contribution to the Ground State Binding-Energy in He-like Uranium

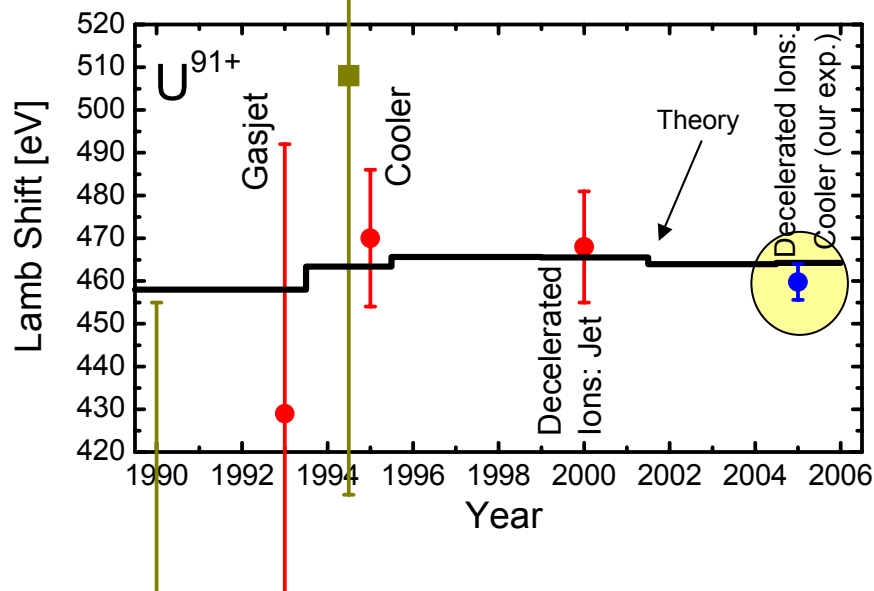


PRECISION TESTS OF BOUND-STATE QED IN EXTREME FIELDS: Lamb shift in H-like uranium measured at the ESR electron cooler



Research Highlights
Nature 435, 858-859

1s Lamb shift



Experiment : 460.2 ± 4.6 eV

Theory : 464.26 ± 0.5 eV



➔ **1% sensitivity to the 1s Lamb shift**

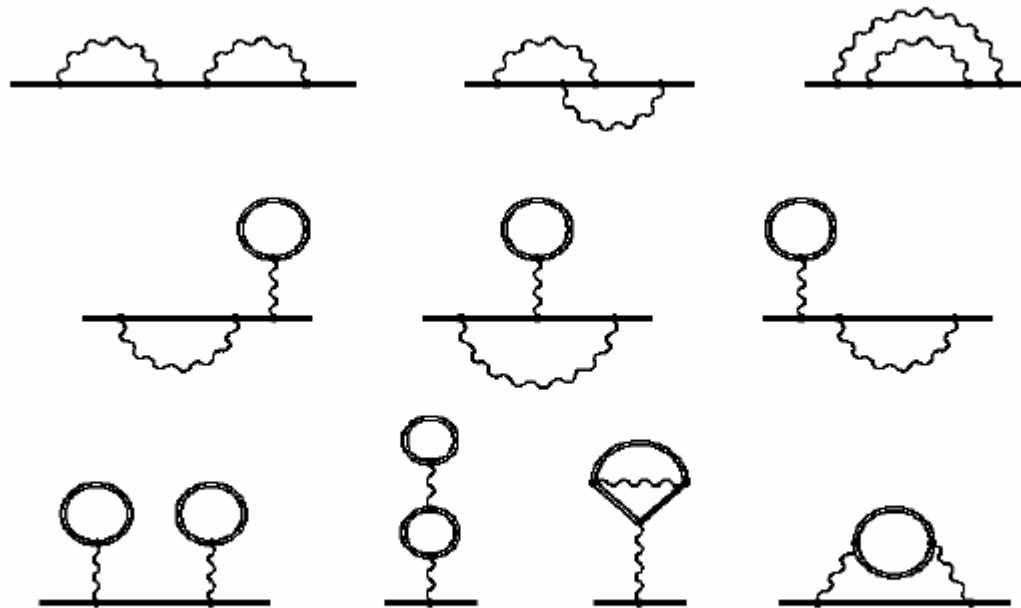
➔ **Most stringent test of bound-state QED
for one-electron high-Z systems**

A. Gumberidze et al., PRL 94, 223001 (2005)
V. A. Yerokhin et al., EPJ D 25, 203 (2003)



QED effects on the energy levels of high-Z few-electron systems

One-electron QED corrections of second order in α
Non-perturbative calculations (in $Z\alpha$)



Goal
~1 eV

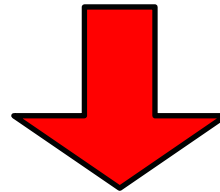
Recent progress: Evaluation of the two-loop self-energy diagrams
(V.A. Yerokhin, P. Indelicato, and V.M. Shabaev, *JETP*, 2005; *PRL*, 2006).



Towards an accuracy of 1 eV

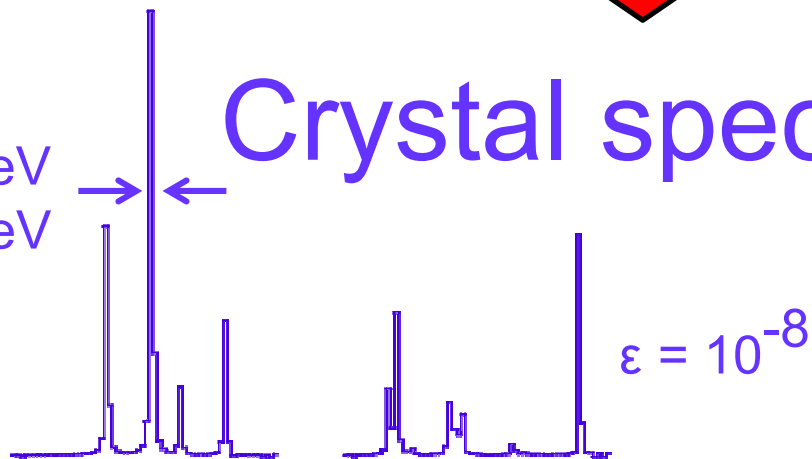
Ge(i) detector

400 eV
at 60 keV



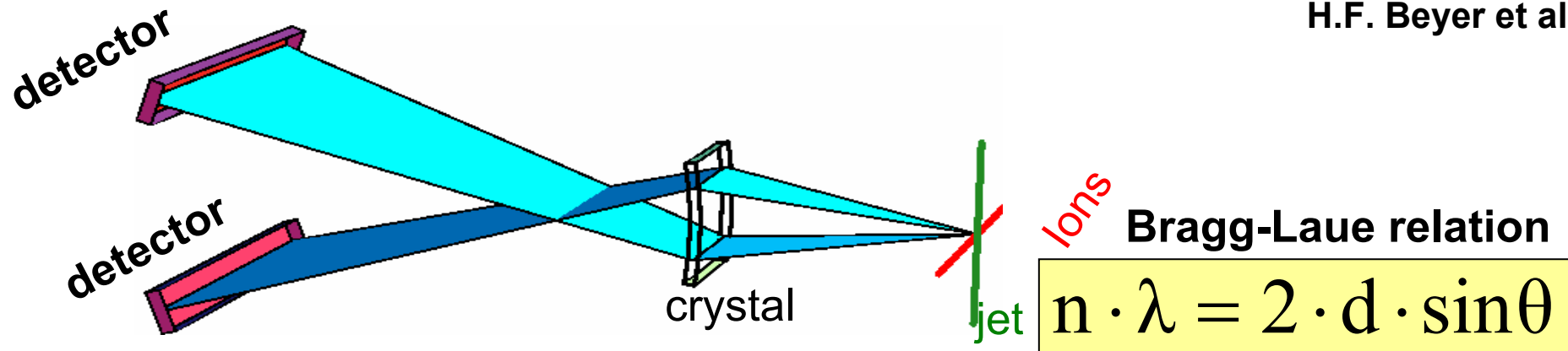
Crystal spectrometer

50-150 eV
at 60 keV



Transmission crystal spectrometer towards an accuracy of 1 eV

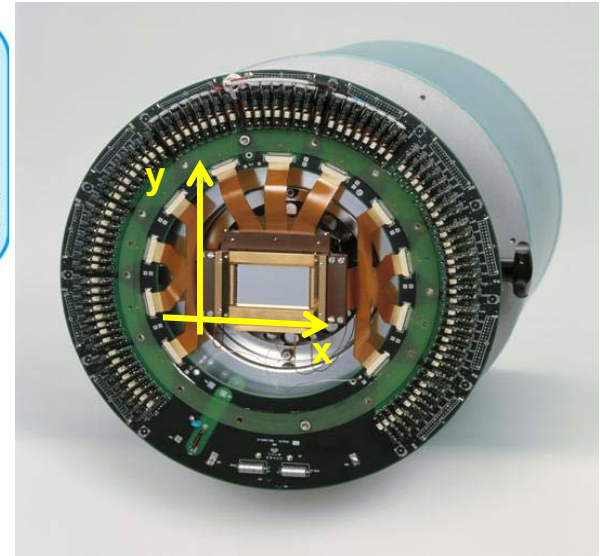
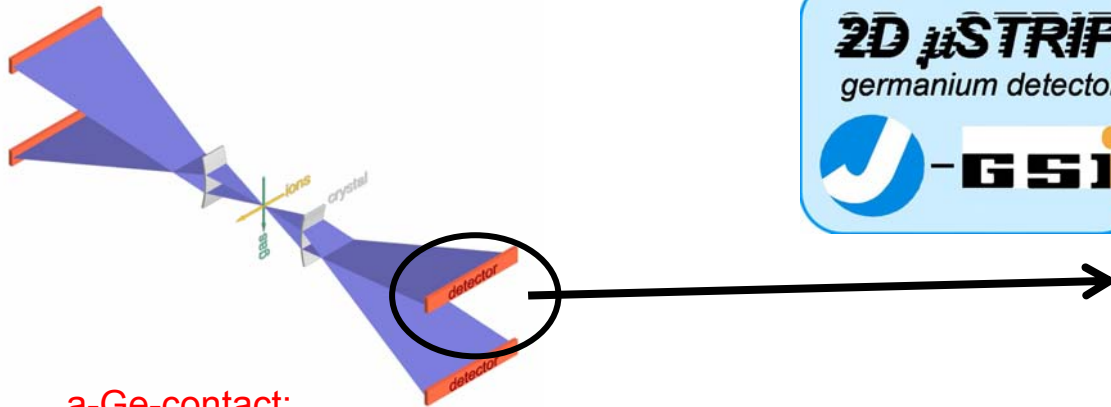
H.F. Beyer et al



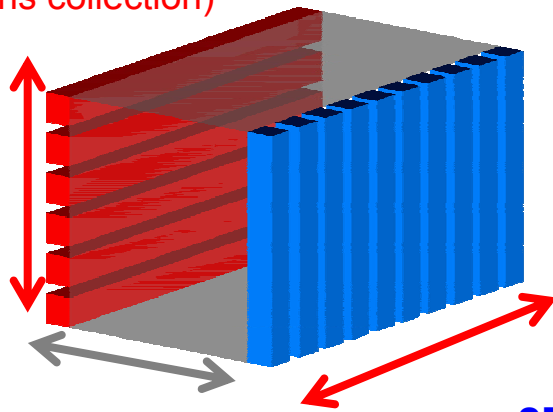
FOCAL spectrometer: $\varepsilon \approx 10^{-8} \Rightarrow 5$ events per hour

~~gas counters (drift chambers)~~

Micro-strip semiconductor detector



a-Ge-contact:
48 strips in the back side
(electrons collection)



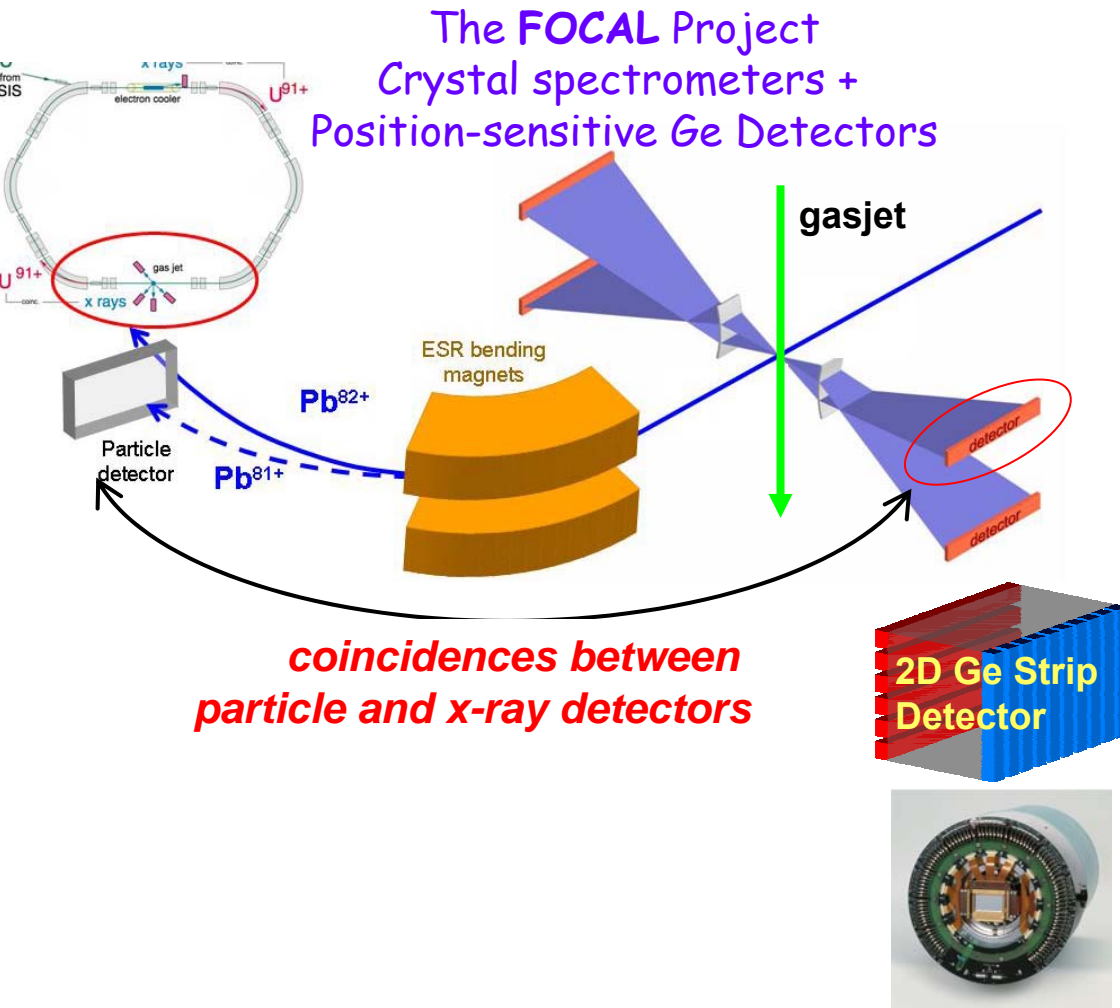
p⁺-contact:
128 strips in the front
side
("holes" collection)

2D detector [1,2]
Ge(i) crystal
128 X 48 Strips
 $\Delta x \sim 1167 \mu\text{m}$
 $\Delta y \sim 250 \mu\text{m} (< 150 \text{ eV})$
 $\Delta E \sim 2.1 \text{ keV}$
 $\Delta t \sim 50 \text{ ns}$

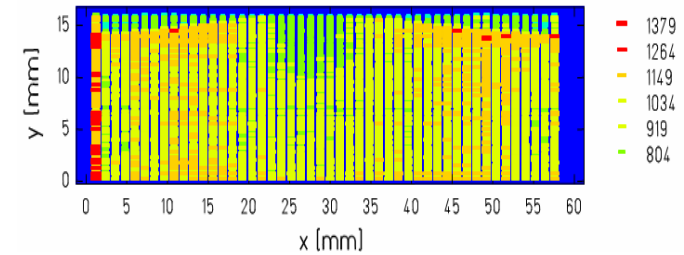
2D/3D position-sensitivity
energy resolution
timing



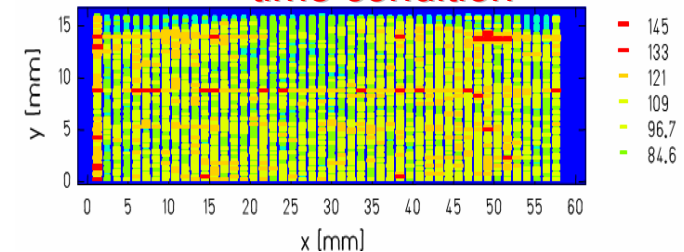
PRECISION TESTS OF BOUND-STATE QED IN EXTREME FIELDS HIGH-RESOLUTION DETECTION DEVICES AT THE ESR



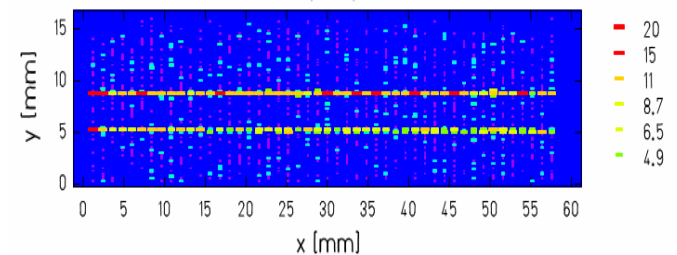
x-ray image (10 keV to 130 keV)



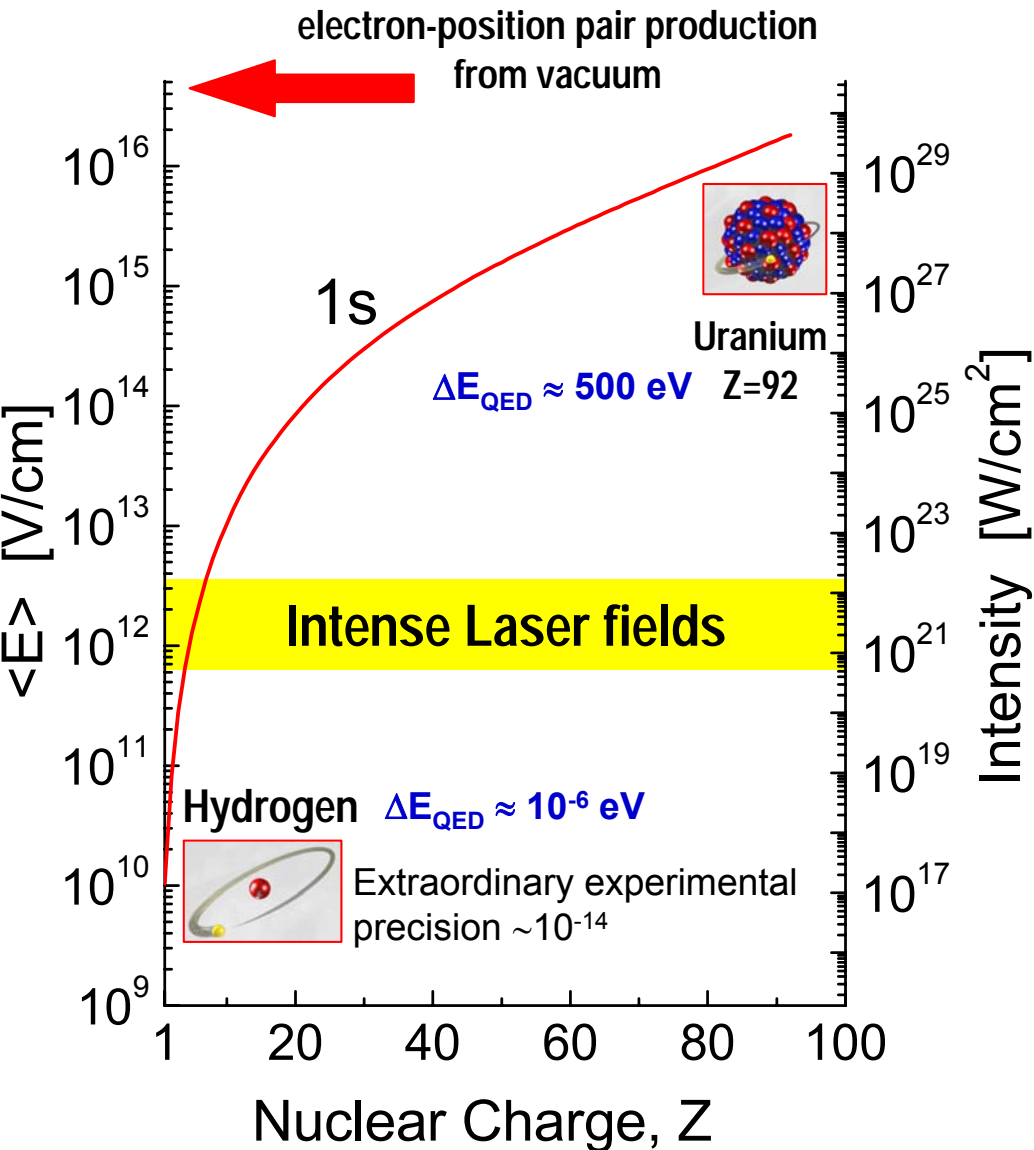
x-ray image (10 keV to 130 keV)
+ time condition



x-ray image (58 keV to 65 keV)
+ time condition



Atomic Physics in Extremely Strong Fields



Atomic Structure at High-Z

- Bound state quantum electrodynamics (QED) in extreme fields
- Effects of relativity on the atomic structure
- Electron correlation in the presence of strong fields

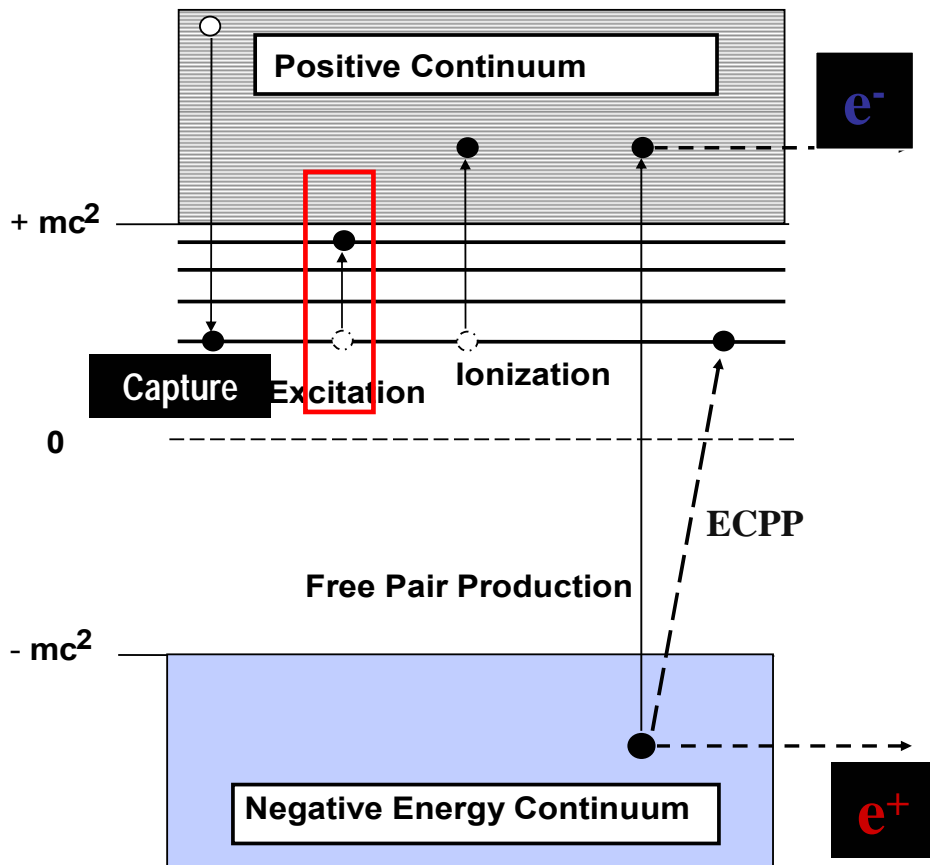
Atomic Collision at High-Z

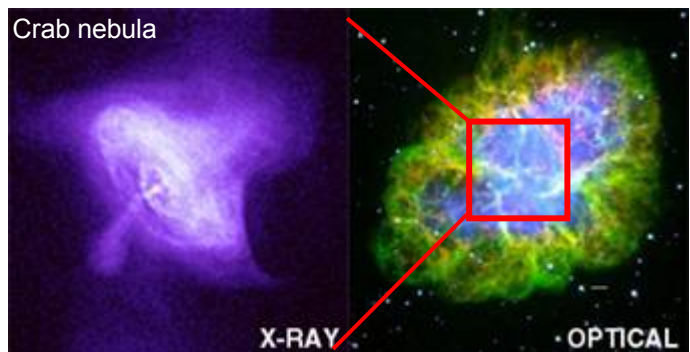
- Correlated many-body dynamics
- Photon matter interaction: e.g., photon polarization effects
- Dynamically induced strong field effects



High- γ

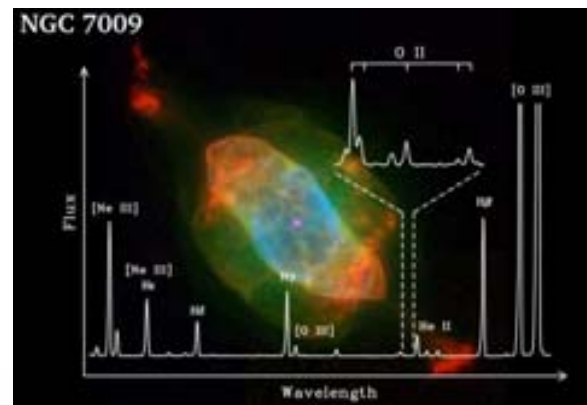
Collision times in the sub-attosecond regime
($10^{-22} \text{ s} < t < 10^{-18} \text{ s}$)



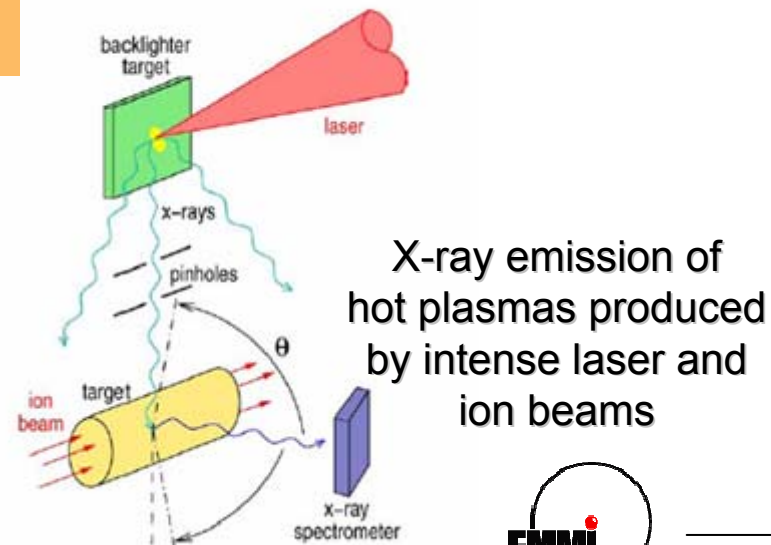
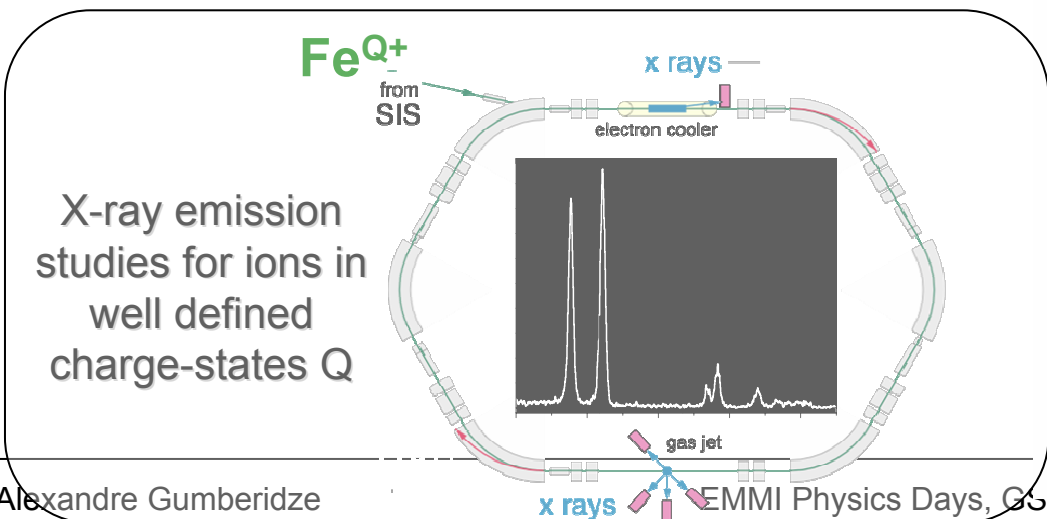


Direct insight into celestial plasmas

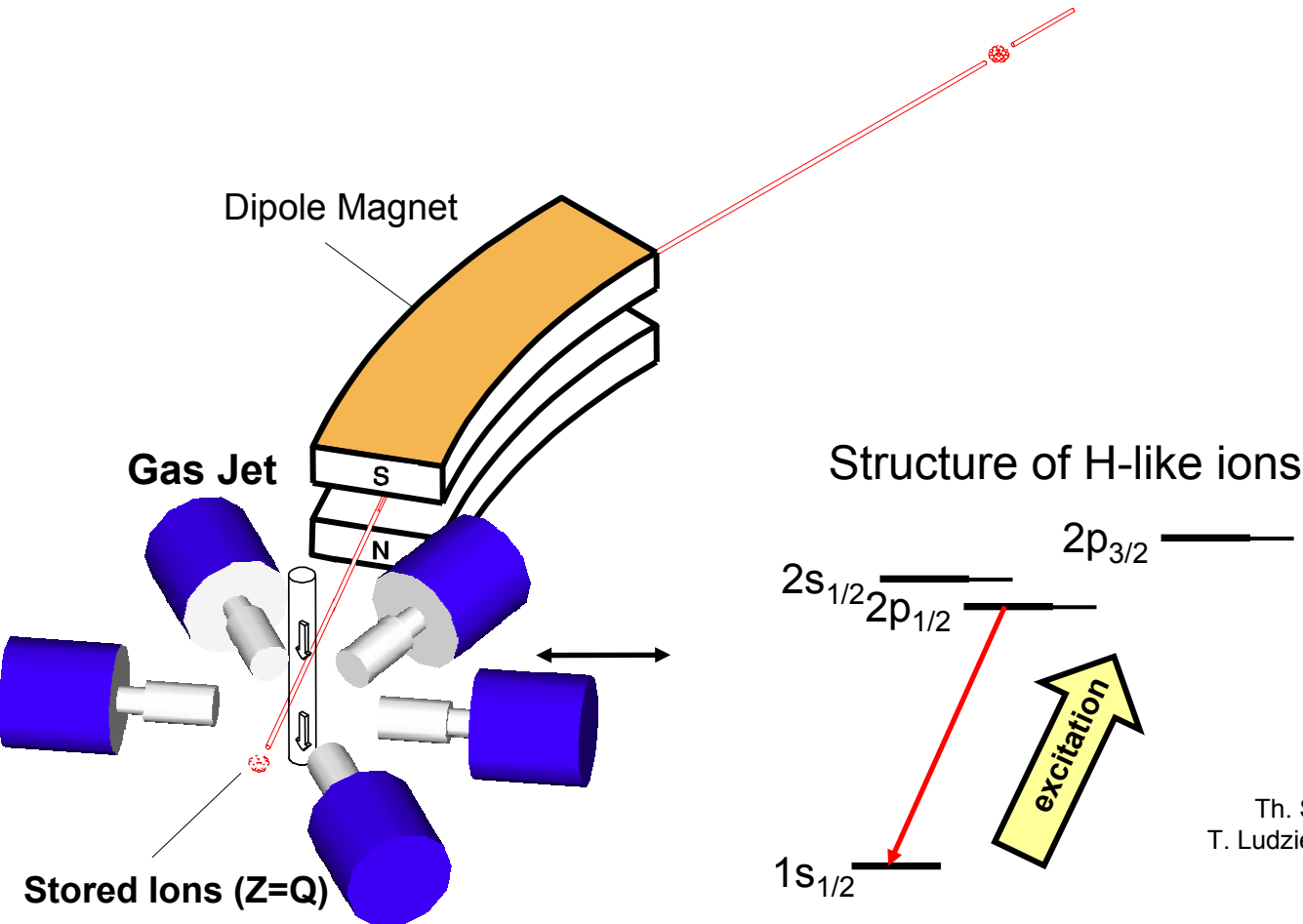
Spectra provide knowledge of temperature, density, element abundance, etc.



Laboratory Astrophysics



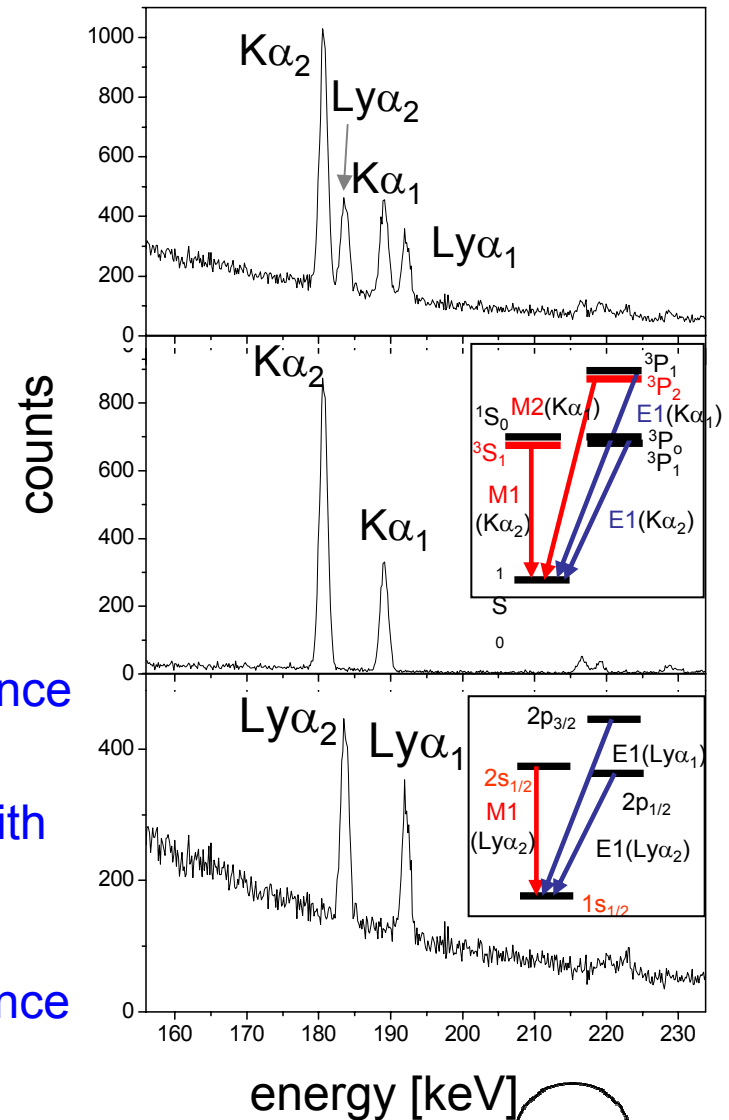
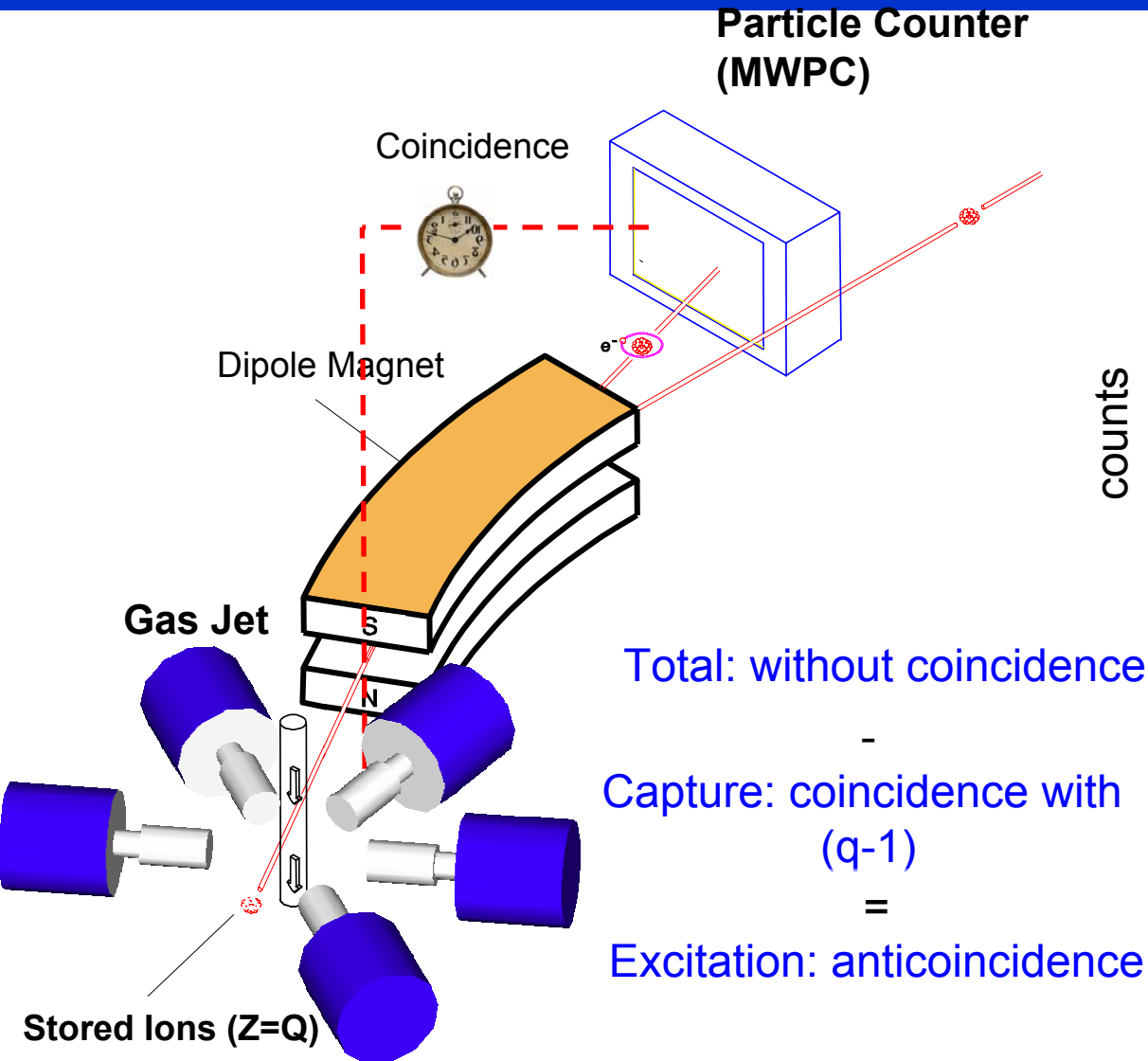
Atomic Dynamics at Strong Fields Explored With HCI at the Supersonic Gas Jet-Target of the ESR



Th. Stöhlker et al *Phys. Rev. A* 57, 845 (1998)
T. Ludziejewski et al *Phys. Rev. A* 61, 052706 (2000)

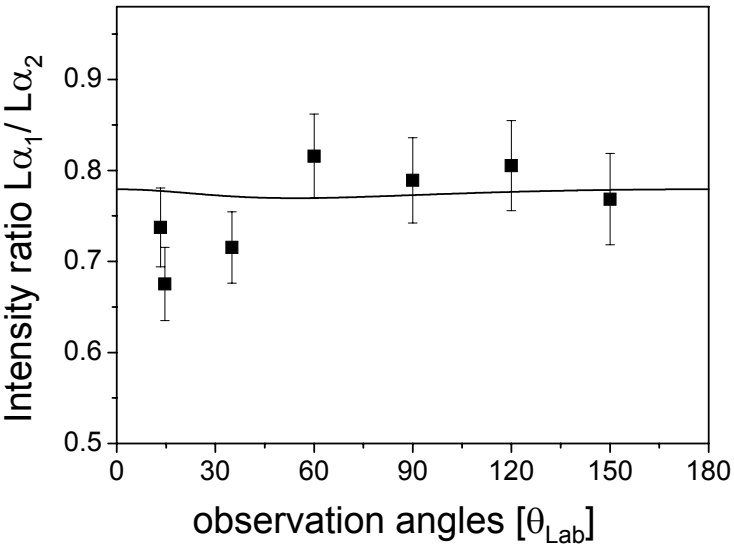


Excitation of H-like uranium in relativistic collisions with various targets



Magnetic sublevel population and alignment: angular differential measurements

$U^{91+} \rightarrow N_2$ @ 220 MeV/u
Excitation



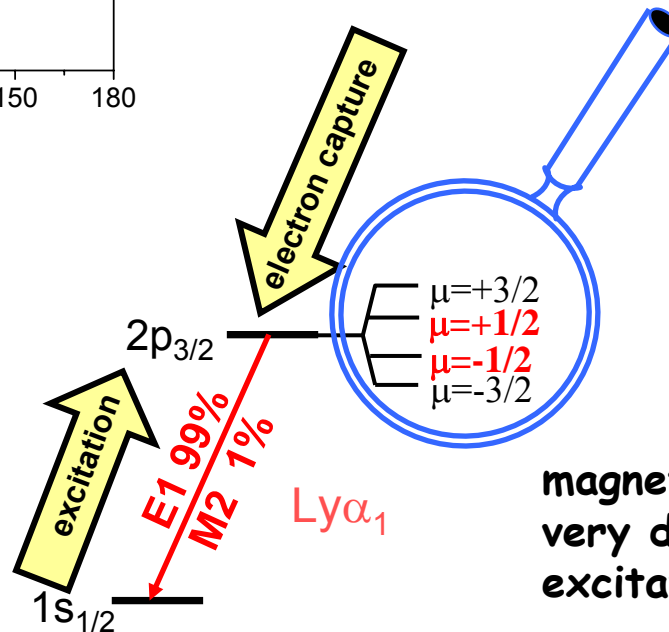
Alignment parameter β_A is zero within the experimental uncertainty

Alignment Parameter

$$\beta_A = \frac{1}{2} \frac{\sigma\left(\begin{smallmatrix} 3 & 3 \\ 2 & 2 \end{smallmatrix}\right) - \sigma\left(\begin{smallmatrix} 3 & 1 \\ 2 & 2 \end{smallmatrix}\right)}{\sigma\left(\begin{smallmatrix} 3 & 3 \\ 2 & 2 \end{smallmatrix}\right) + \sigma\left(\begin{smallmatrix} 3 & 1 \\ 2 & 2 \end{smallmatrix}\right)}$$

$Ly\alpha_2$ ($2p_{1/2} - 2s_{1/2}$) is Identically isotropic

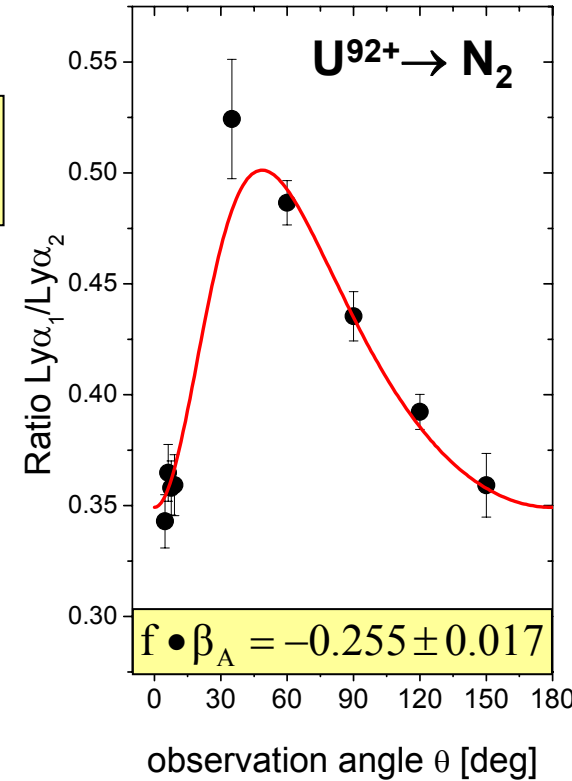
$$W(\theta) \propto 1 + f \left(\frac{a_{M2}}{a_{E1}} \right) \cdot \beta_A \cdot \left[1 - \frac{3}{2} \sin^2 \theta \right]$$



magnetic sublevels are populated very differently by Coulomb excitation and REC

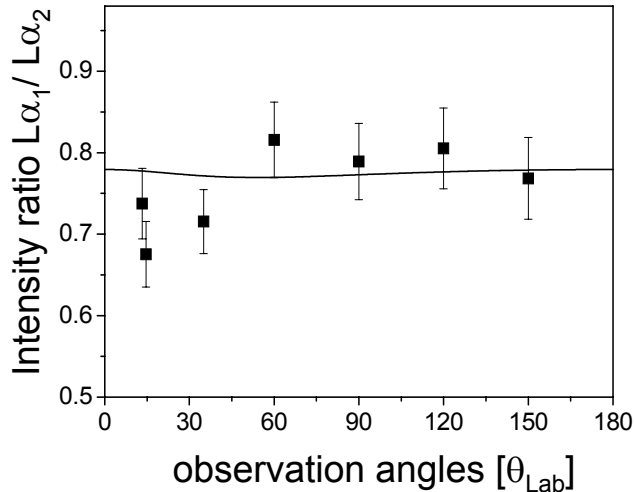
REC

Th. Stöhlker, et al., PRL 79, 3270 (1997)

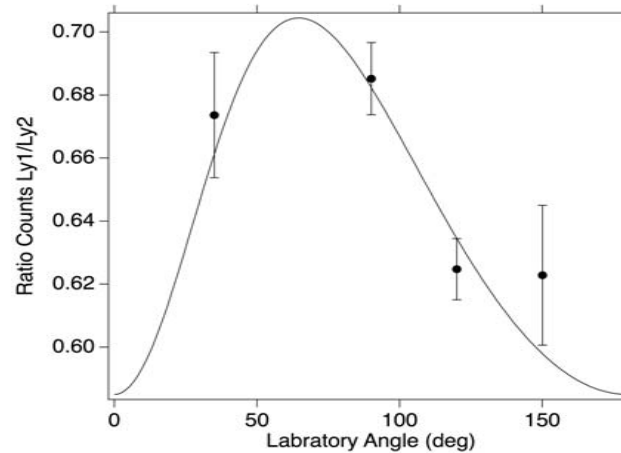


Magnetic sublevel population and alignment produced by excitation for different targets and different energies

$U^{91+} \rightarrow N_2 @ 220 \text{ MeV/u}$

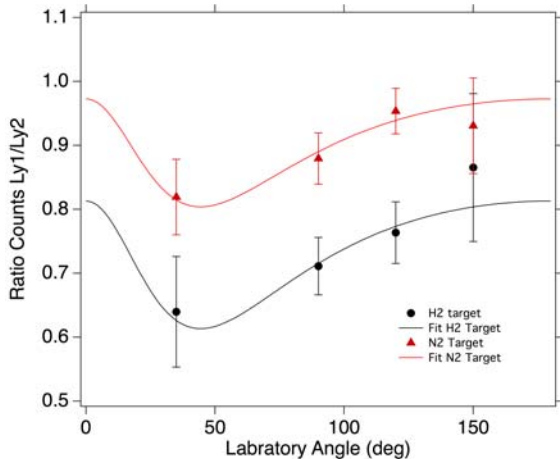


$U^{91+} \rightarrow N_2 @ 100 \text{ MeV/u}$

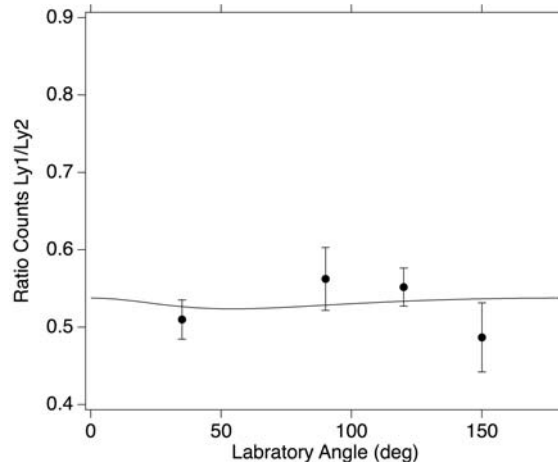


Magnetic sublevel population changes significantly with the collision energy

$U^{91+} \rightarrow H_2, N_2 @ 400 \text{ MeV/u}$



$U^{91+} \rightarrow H_2 @ 220 \text{ MeV/u}$



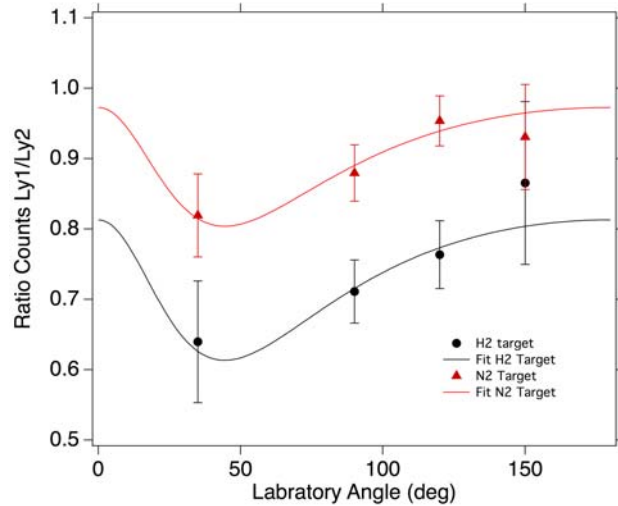
It seems not to be affected by change of the target. This is not the case for relative differential cross-section



Magnetic sublevel population and alignment produced by excitation for different targets and different energies

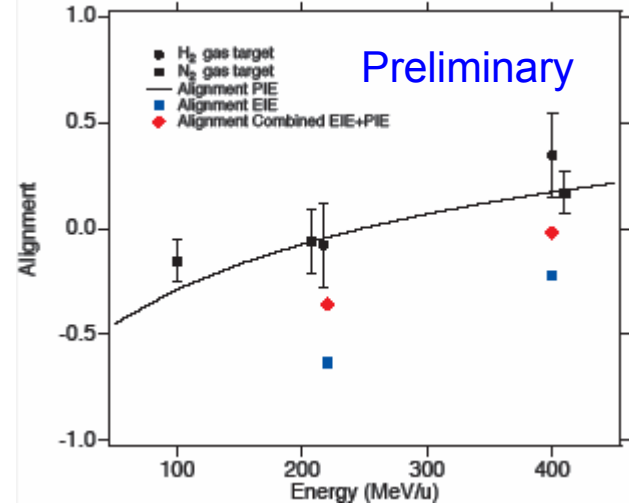
Excitation by the nuclear field scales as Z^2 . EIE scales as Z .
changing the target \rightarrow change the relative contribution of the two processes

$U^{91+} \rightarrow H_2, N_2 @ 400 \text{ MeV/u}$



influence of EIE

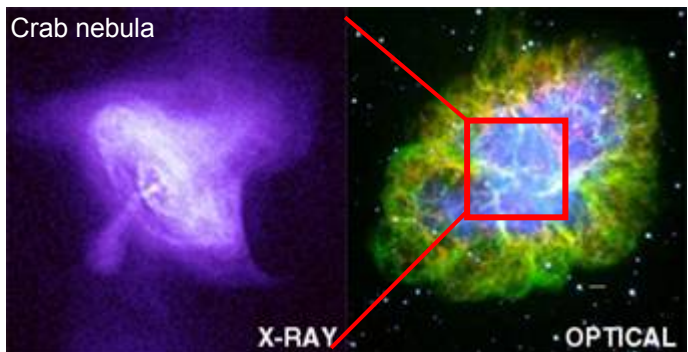
$U^{91+} \rightarrow H_2$



calculations by A. Surzhykov et al

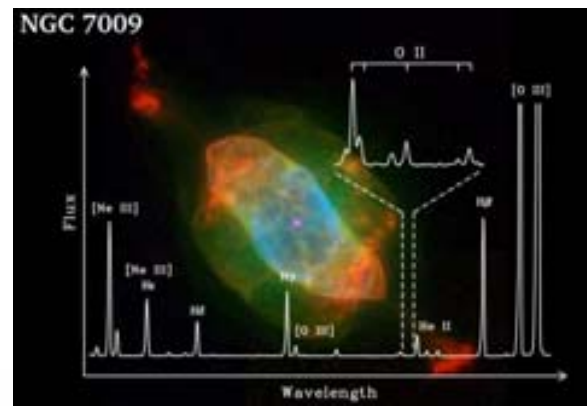
EIE calculations by C. J. Fontes et al





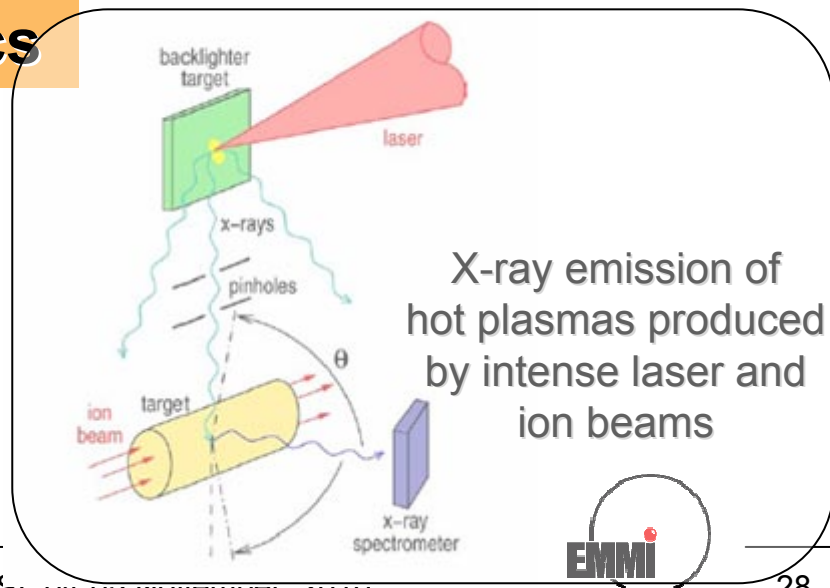
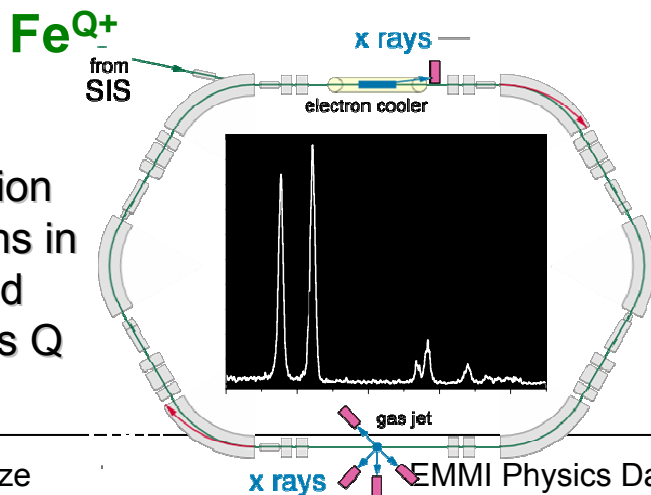
Direct insight into celestial plasmas

Spectra provide knowledge of temperature, density, element abundance, etc.



Laboratory Astrophysics

X-ray emission studies for ions in well defined charge-states Q



X-ray emission of hot plasmas produced by intense laser and ion beams



Hard X-Ray Inner-Shell Spectra Produced by Intense Picosecond Laser Pulses and Recorded by Cauchy Type Spectrometers

Exploiting Atomic Physics techniques for Exploring Plasmas Generated

by High-power Laser

Goals and motivation

- High-energy plasma diagnostics: temperature, density, ionization balance, opacity.
- **Hot electron energy distribution, hard x-ray brightness optimization**
- Conversion efficiency of Laser power to hard x-rays



LULI pico2000 Facility

- Nd:glass laser, wave length: $1,053\mu\text{m}$
- Long pulse beam: 1kJ, 1.5 ns
- Short pulse beam: 200 TW - 200 J in 1 ps



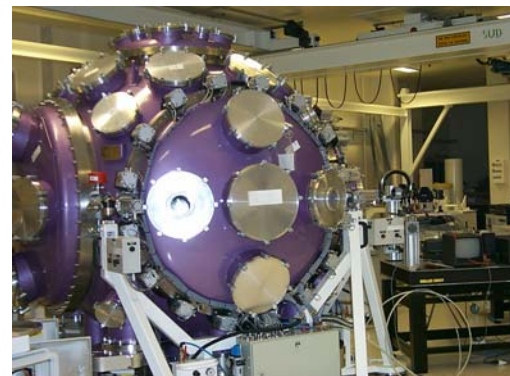
laser hall



capacitors bank



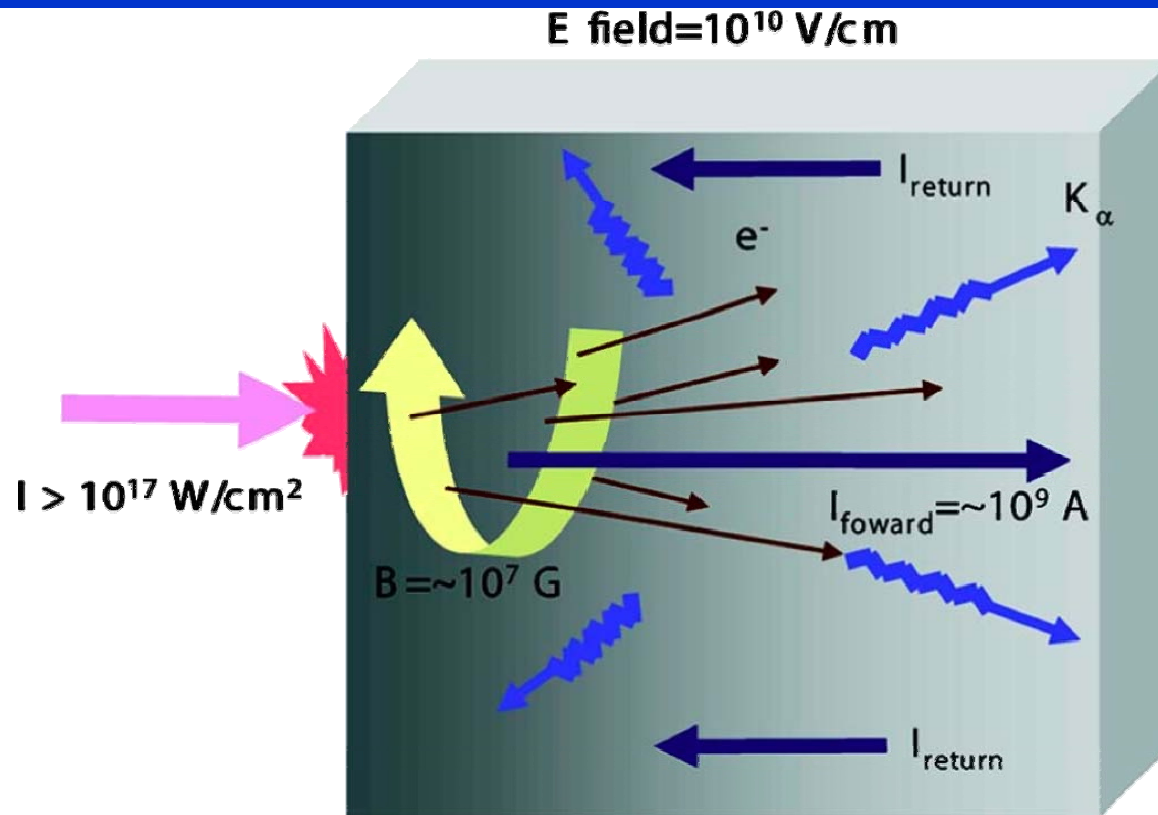
pico2000
compression
chambers



MILKA
target
chamber

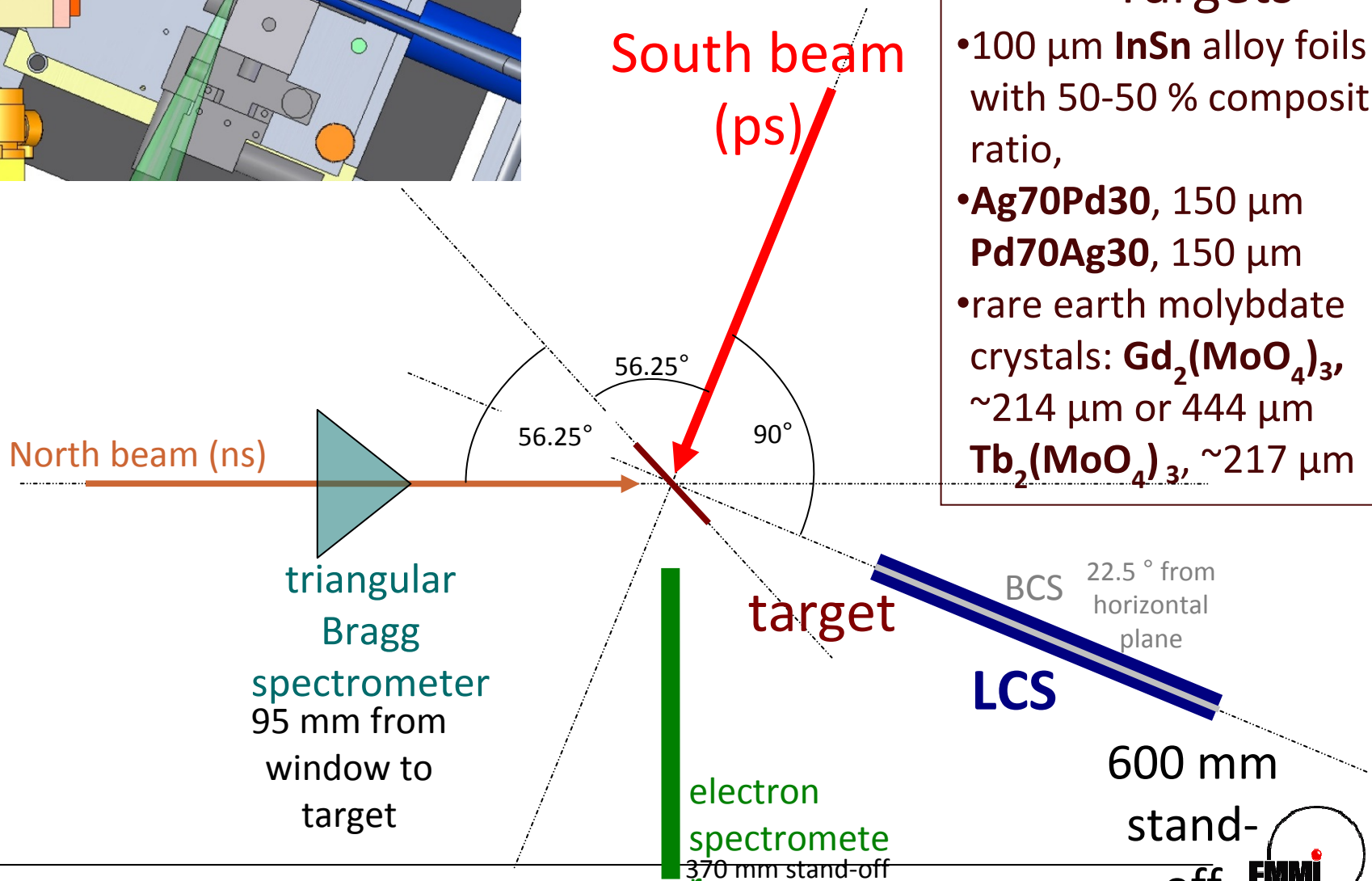
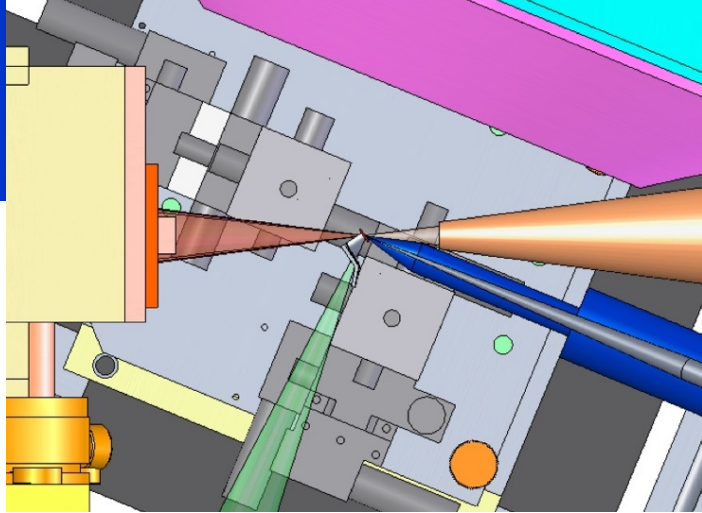


Schematic of $K\alpha$ Production Mechanism



The high-intensity laser with $I \geq 10^{17} \text{ W/cm}^2$ creates superthermal to relativistic hot electrons. These hot electrons travel through the target material while producing $K\alpha$ and Bremsstrahlung photons. Because of the self-generated electric fields from the ions, the hot electrons reflux at the material boundary, creating more photons. This mechanism is known to be a much more efficient way of generating high-energy photons $>10 \text{ keV}$ compared to thermally driven transitions.

Experimental Setup

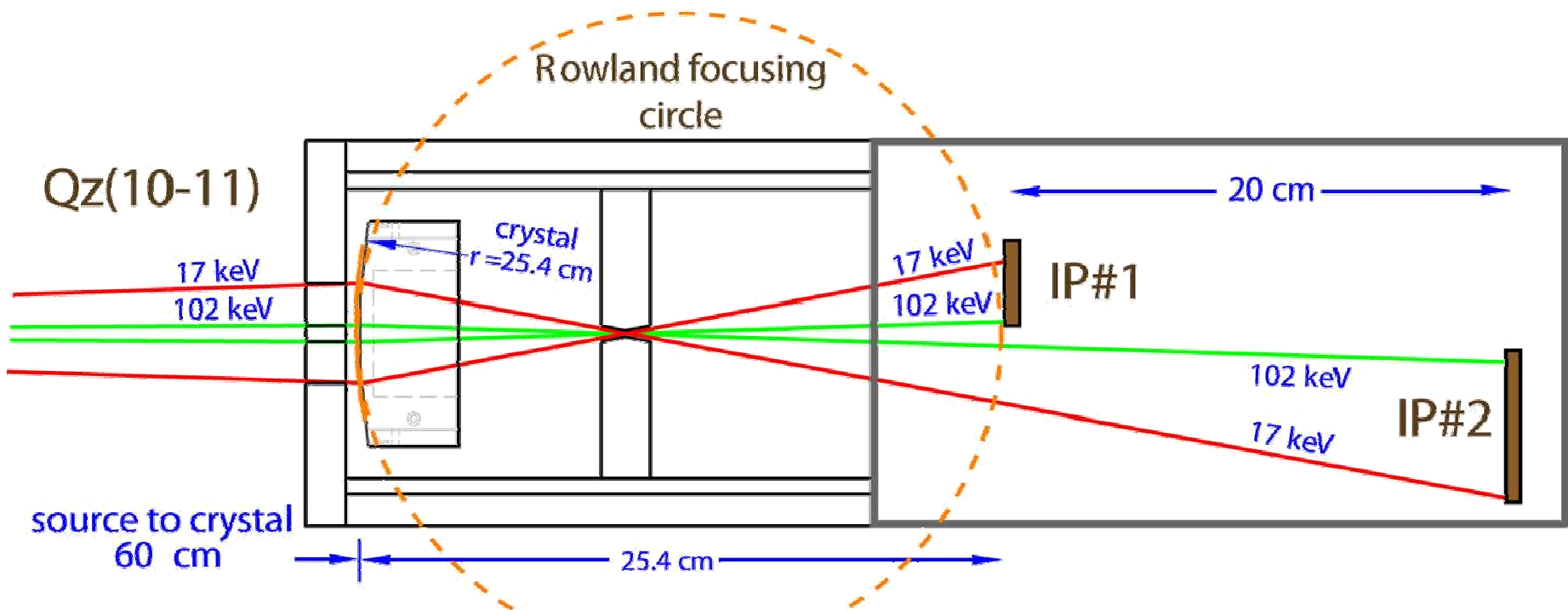


Targets

- 100 μm InSn alloy foils with 50-50 % composition ratio,
- Ag70Pd30, 150 μm
Pd70Ag30, 150 μm
- rare earth molybdate crystals: $\text{Gd}_2(\text{MoO}_4)_3$, $\sim 214 \mu\text{m}$ or $444 \mu\text{m}$
 $\text{Tb}_2(\text{MoO}_4)_3$, $\sim 217 \mu\text{m}$

LULI Crystal Spectrometer (LCS)

Built by a team from the Naval Research Laboratory (NRL) and the National Institute of Standards and Technology (NIST)



- ❖ 250 μm thick Qz(10-11) crystal bent to a cylinder with the radius of 254 mm
- ❖ Two detector positions:
 - ❖ 1) on the focusing Rowland circle
 - ❖ 2) 200 mm off the Rowland circle to increase resolution for point source Seely J. F. et al. Appl. Opt. 47 p.2767 (2008)
- ❖ Source to crystal stand off distance: 600 mm

The FOCAL Crystal spectrometers together with Position-sensitive Ge Detectors

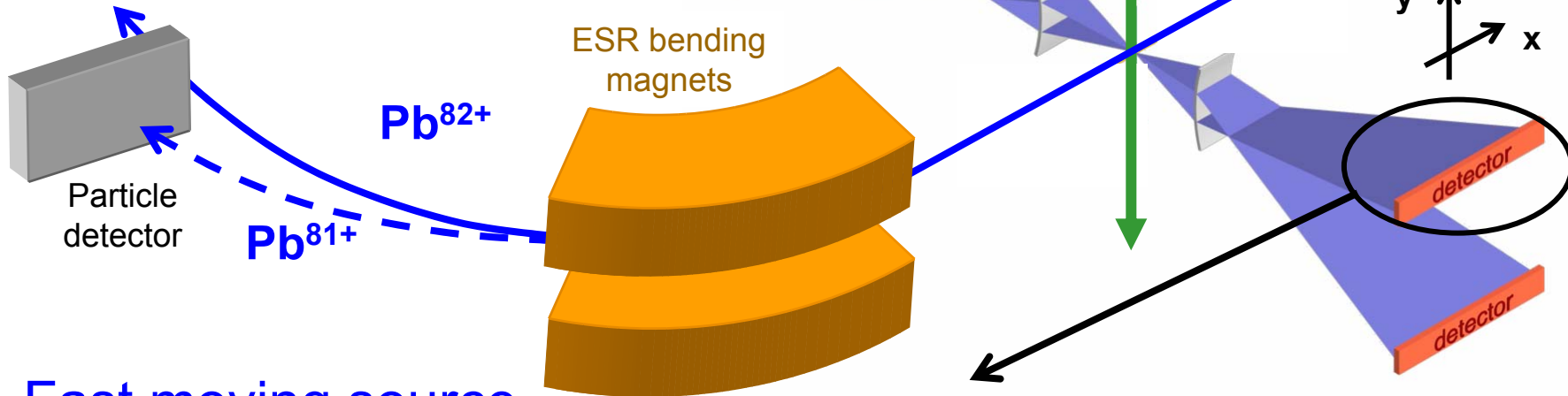
FOCAL Laue crystal spectroscopy [1]

- Transmission Bragg spectrometer
- Theoretical resolution: ~ 50 eV @ 60 keV
- Bent crystal \rightarrow focusing properties
- Efficiency: 10^{-8}

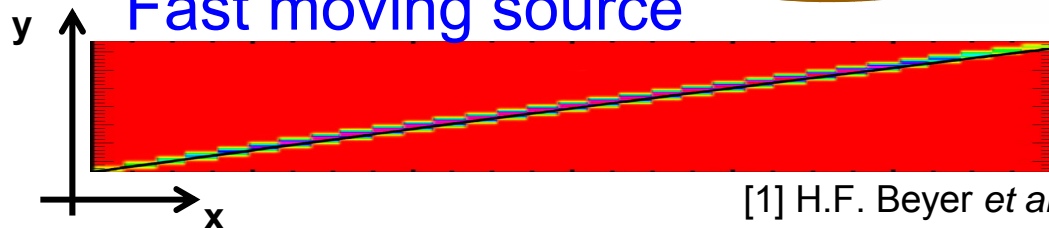
Lead 1s Lamb shift Experiment

Jet target
 supersonic krypton jet
 density: $\sim 10^{12}$ atoms/cm²
 width: ~ 5 mm

Ion beam
²⁰⁸Pb⁸²⁺ ion beam
 energy: 210 MeV/u
 $\beta = 0.586$ (\rightarrow 58% of c)



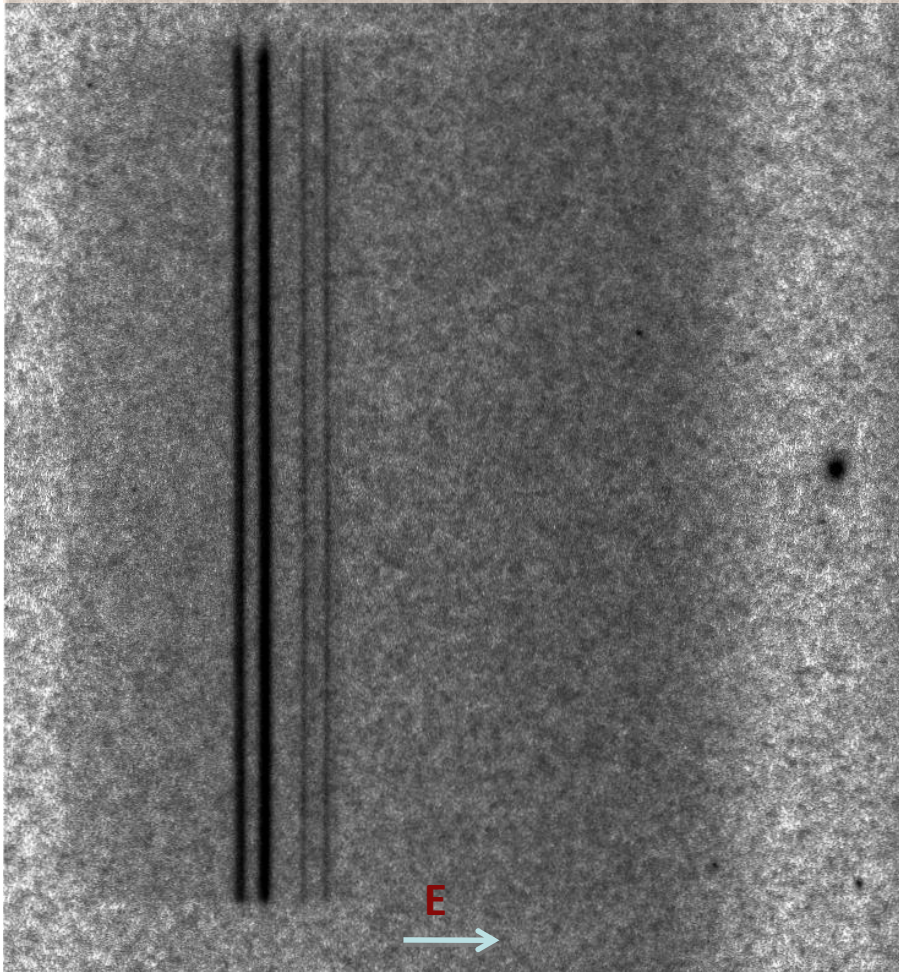
Fast moving source



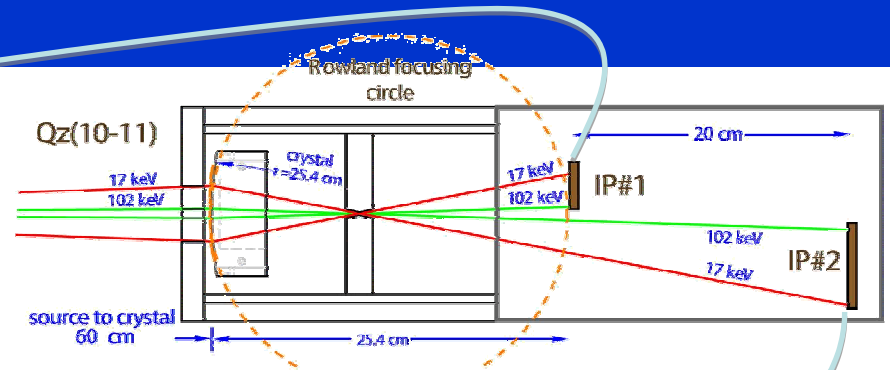
[1] H.F. Beyer *et al.*, Spectrochim. Acta, Part B **59**, 1535-1542 (2004).

Sample Spectral Image Registered with LCS

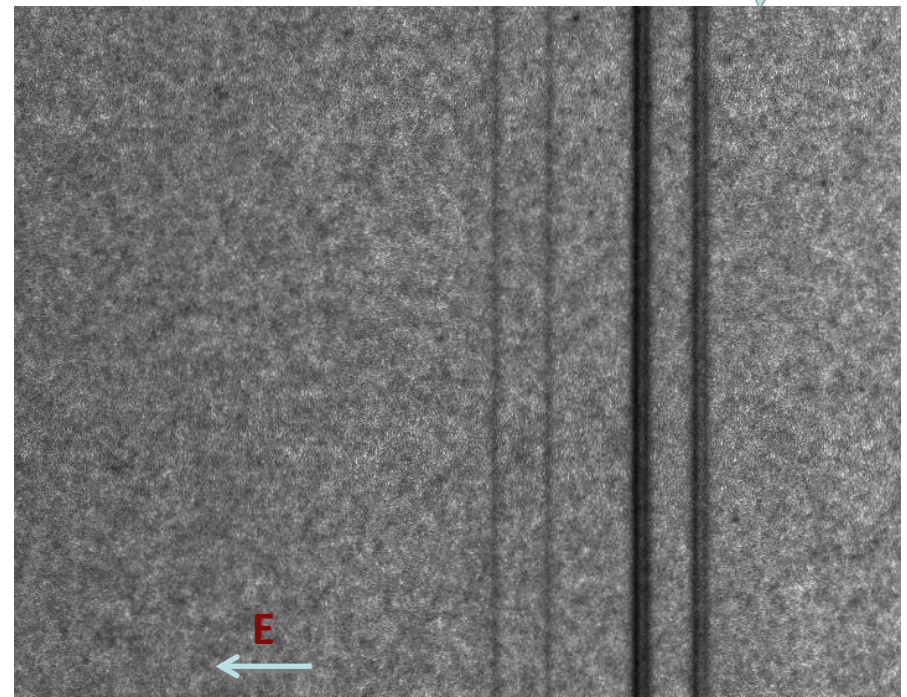
S03 LCS_A,
Target: Ag70Pd30 alloy foil, 150 μm



Laser Energy: 85 J
1 ps, focused

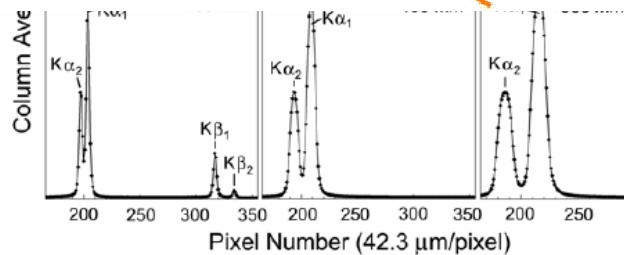
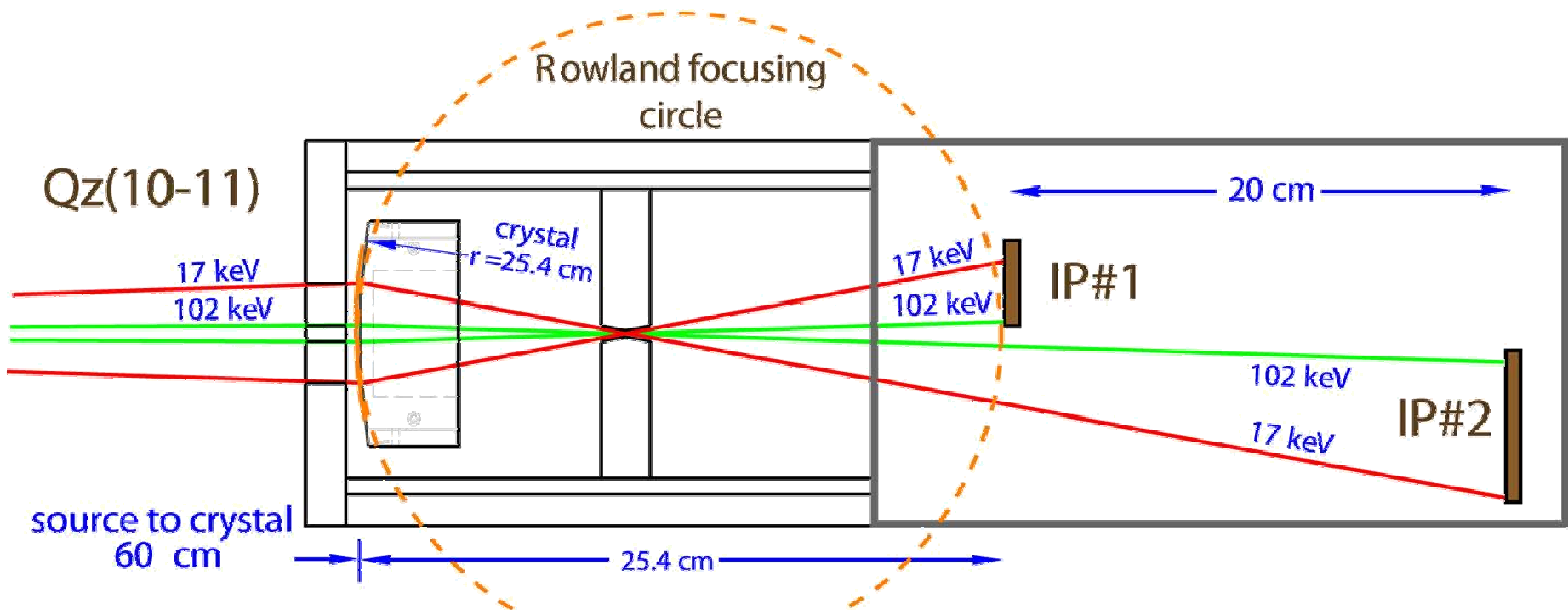


Fuji MS image plates

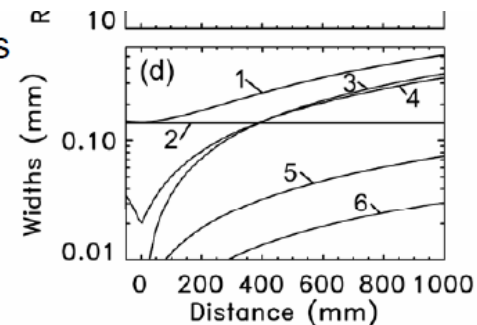


Ag Pd Ag Pd
K β K β K α EMMI

Energetic Electron Propagation Range: Source broadening of the spectral lines

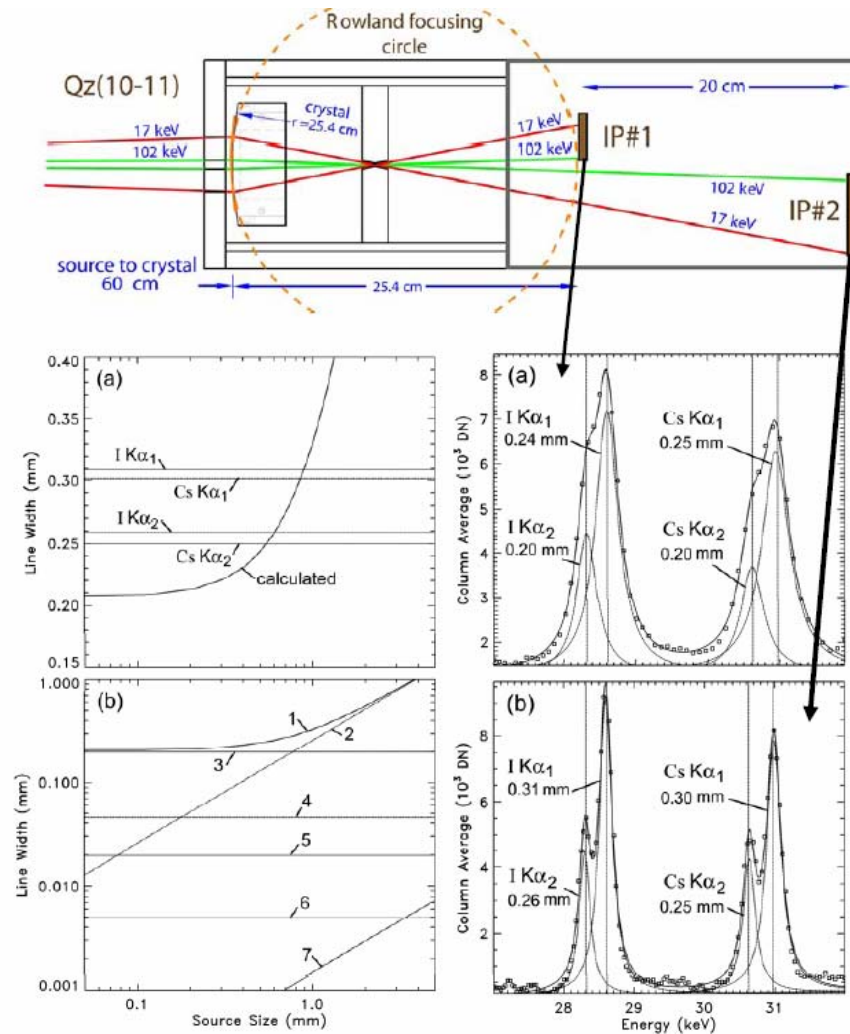


- 4 – Crystal thickness
- 5 – Natural width
- 6 – Crystal rocking curve
- 7 – Aberrations
(very small)



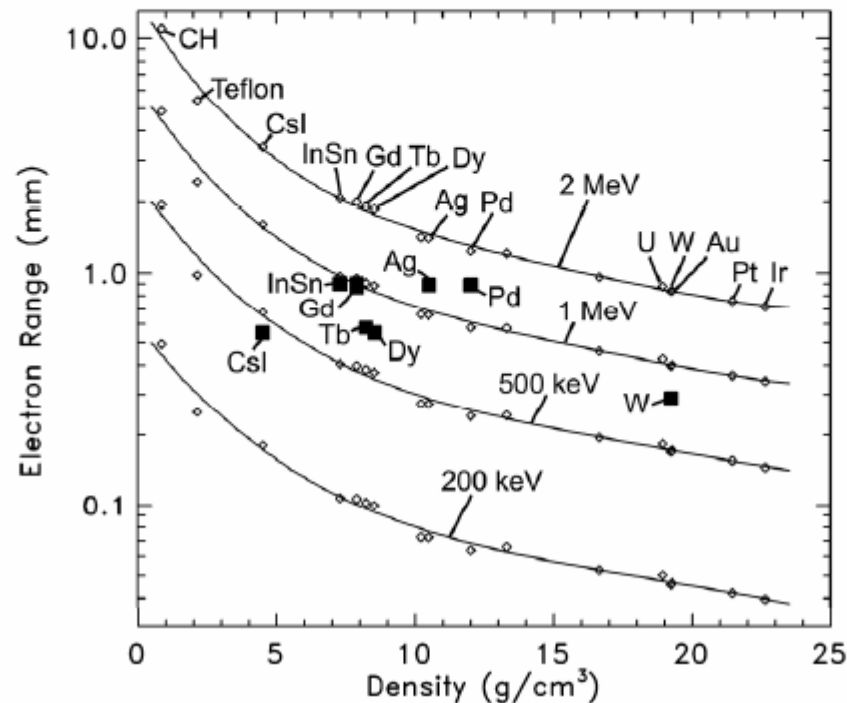
LULI ps Laser X-ray source size

- LULI laser: 100 J, 1 ps, 10 μm focal spot, 10^{20} W/cm² focused intensity.
- Spectra were recorded by placing two MS image plates on the RC (detector broadening) and 20 cm behind the RC (source broadening).
- Comparisons with a geometrical model of the spectrometer indicate x-ray source size up to 1 mm.
- Energetic electrons generated in the focal spot propagate into the cold solid material beyond the focal spot and produce characteristic K-shell lines.

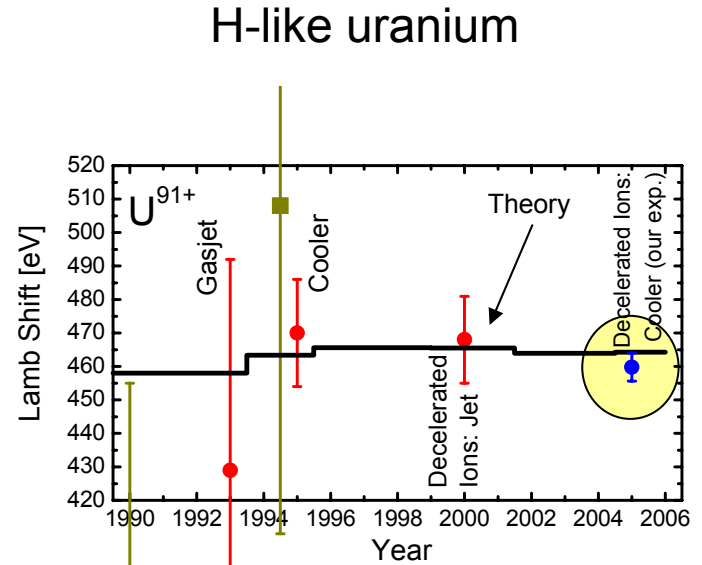
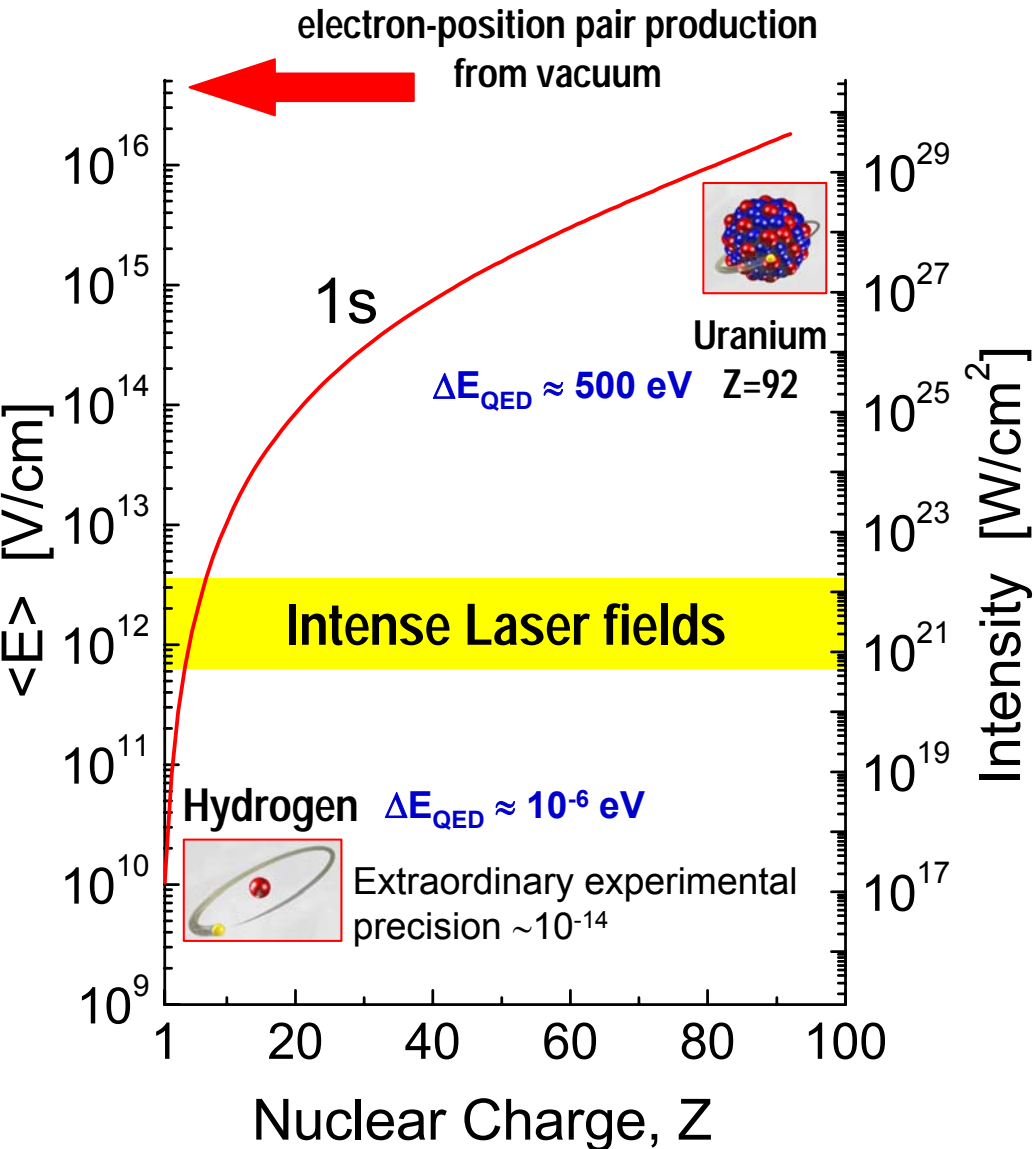


Electron Ranges Measured from Line Broadening

- The range in electrically resistive CsI is relatively smaller than in highly conducting Ag and Pd.
- This suggests that energetic electron propagation in the resistive material is inhibited by the resistive electric force (lower return current).

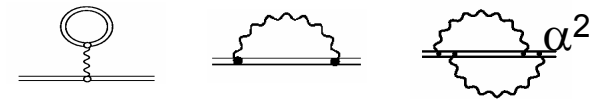


Atomic Physics in Extremely Strong Fields



Experiment (Gumberidze et al., PRL 2005): $460.2 \pm 4.6 \text{ eV}$

Theory (Yerokhin et al., PRL 2003): $464.26 \pm 0.5 \text{ eV}$

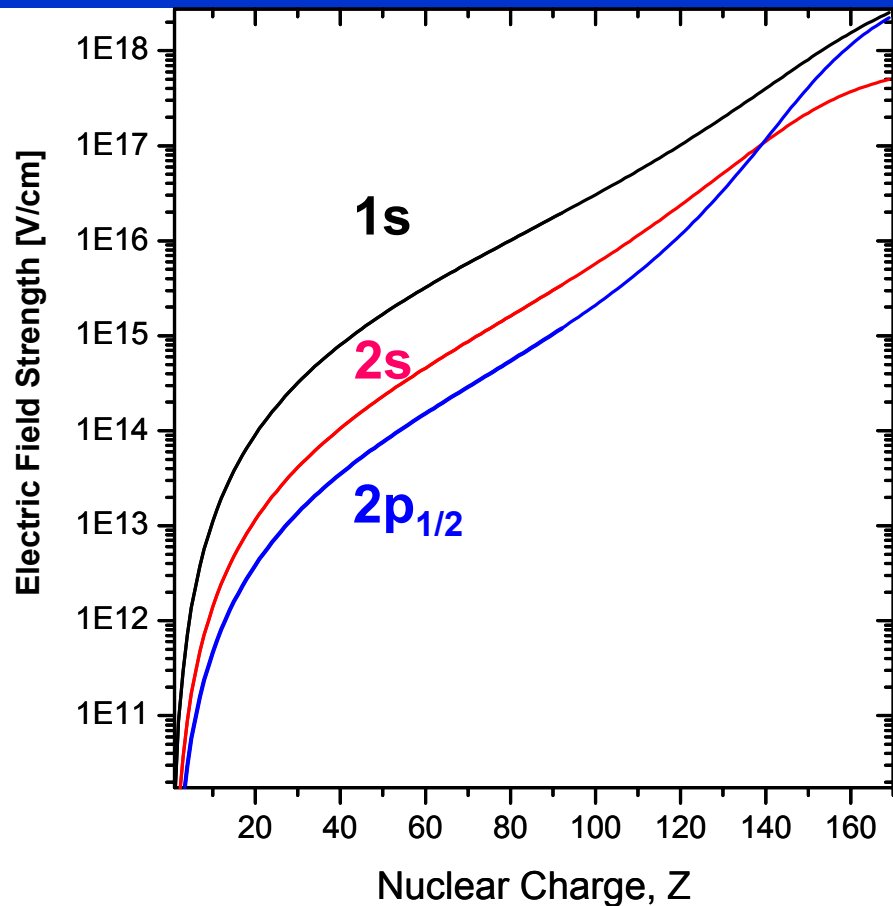


➔ 1% sensitivity to the 1s Lamb shift

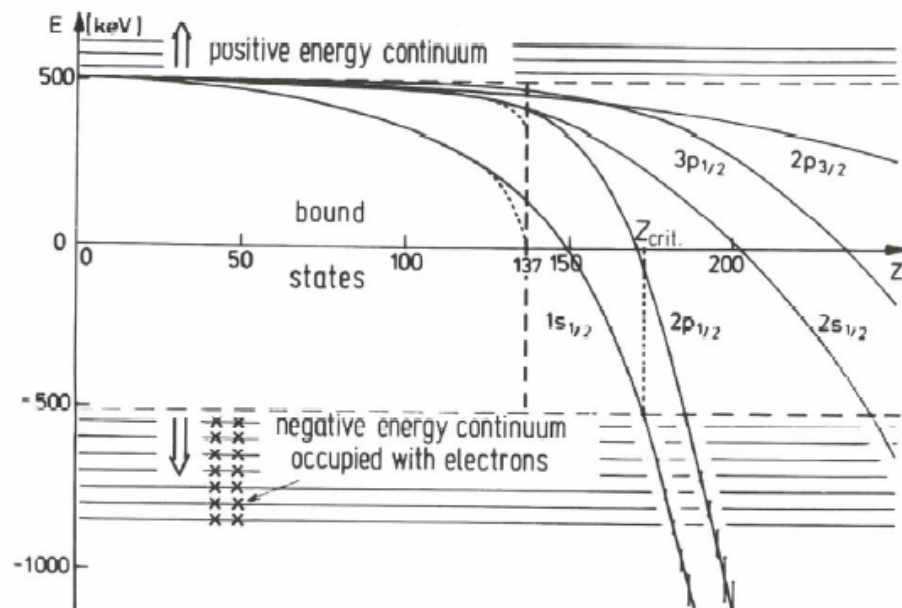
➔ stringent test of bound-state QED for one-electron high- Z systems



Critical- and Super-Critical Fields

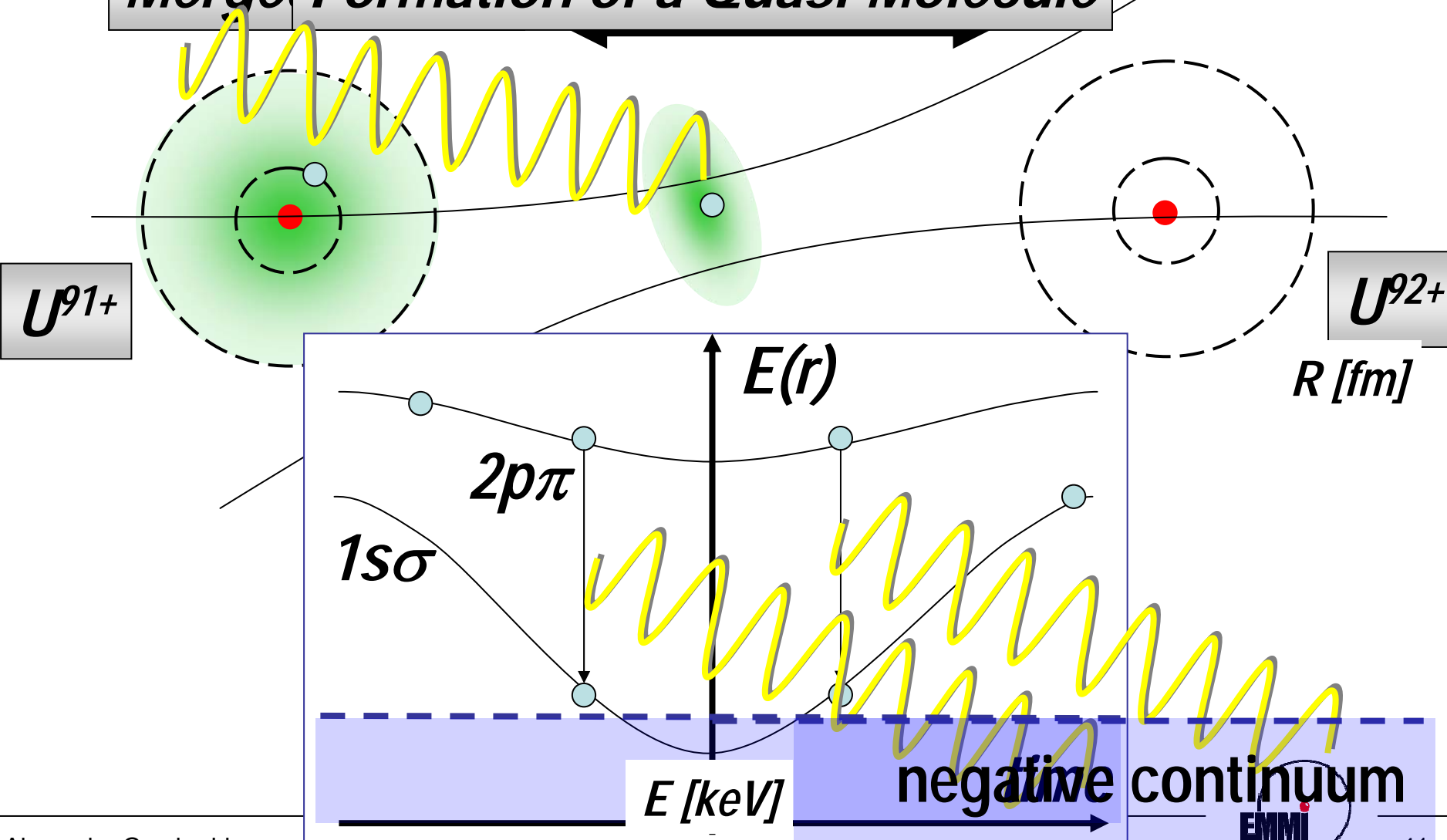


spectroscopy of the inner shells in superheavy quasimolecule systems with energy eigenvalues in the vicinity of the negative continuum



Quasimolecules

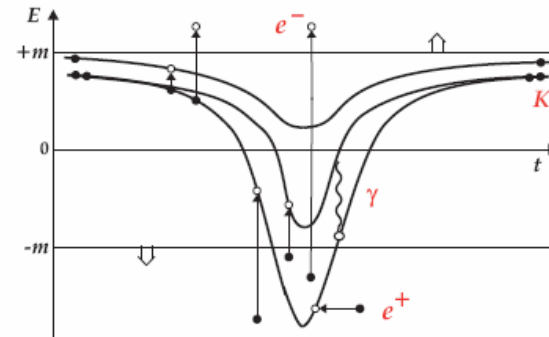
Merge Formation of a Quasi-Molecule



Various Processes and Experimental Observables

In systems with $(Z_1 + Z_2) > 137$:

“Collapse” of wave functions leads to strong $\partial/\partial R$ couplings (between $\kappa = \pm 1$ states). *Multi-step processes* become important.



• K-hole production

High ionisation rates: $P_{1s\sigma} \simeq 10\%$.

Approximate scaling behaviour:

$$P_{1s\sigma}(b) \simeq D(Z) e^{-2R_{\min}q_{\min}} \quad \text{where} \quad q_{\min} = \frac{E_{1s\sigma}^B(R_{\min})}{\hbar v_{\text{ion}}} \quad (\text{minimum momentum transfer})$$

→ “Spectroscopy” of superheavy quasimolecules.

• δ -electron production

The high-energy tail (up to $E_e > 2$ MeV) probes the high-momentum components of the the quasimolecular wave functions.

• Quasimolecular X rays (MOX)

Broad photon spectra. No “end point”, quasistatic picture not applicable.

• Positron creation

• Drastic increase of positron yield with nuclear charge Z :

$$P_{e^+} \propto Z^{20}$$

• *No qualitative signal* for level diving expected. (*Collisional broadening*)

• Good quantitative agreement with experiments: $P(b)$, $P(Z)$, dP/dE_{e^+} .

Early MO Studies Using Solid Targets

Single-pass experiments

1972: Mokler, Stein and Armbruster, **X Rays from Superheavy Quasiatoms Transiently Formed during Heavy Ion-atom Collisions** PRL 29.

1974: Kraft, Mokler and Stein, **Anisotropic Emission of Noncharacteristic X Rays from Low-Energy I-Au Collisions**, PRL 33.

1978: Liesen, Armbruster, Behncke, and Hagmann, **4.7 MeV/u Xe-Au impact parameter measurements of K-shell vacancy production**, Z. Physik A 288.

1979: Kozhuharov et al., **1.4 GeV U-Pb and Pb-Pb positron production, impact parameter measurements for $b < 40\text{fm}$** , PRL 42.

1983: Maor, Liesen, Mokler, Rosner, Schmidt-Böcking and Schuch, **impact parameter measurements for 1.4 MeV/u Ni-Zr,Ag,Te,Au collisions**, PRA 27.

1983: L. Tserruya et al. **Interference Effects in the Quasimolecular K X-Ray Production Probability for 10-MeV Cl^{16+} -Ar Collisions** Phys. Rev. Lett. **50**, 30

1983: P. Armbruster, **Heavy ion collision induced characteristic x-ray production – cross section experiments**, in W. Greiner (ed.) Quantum electrodynamics of strong fields, Plenum Press, New York,, p. 135.

F. Bosch, **Experiments on the excitation of the innermost electrons in extremely strong fields**, ibidem, p.155

1984: P. H. Mokler and D. Liesen, **X-rays from superheavy collision systems**, in H. J. Beyer and H. Kleinpoppen (eds.) Progress in atomic spectroscopy, Part C, Plenum Press, New York and London,, p.321

H. Backe and Ch. Kozhuharov, **Investigations of superheavy quasiatoms via spectroscopy of δ rays and positrons** ibidem, p.459

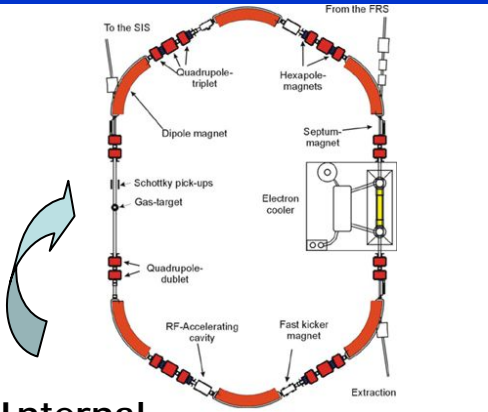
1985: R. Anholt, **X-rays from quasimolecules** Rev. Mod. Phys. 57, 995.

1988: R. Schuch et al., **Quasimolecular x-ray spectroscopy for slow Cl^{16+} -Ar collisions** Phys. Rev. A **37**, 3313

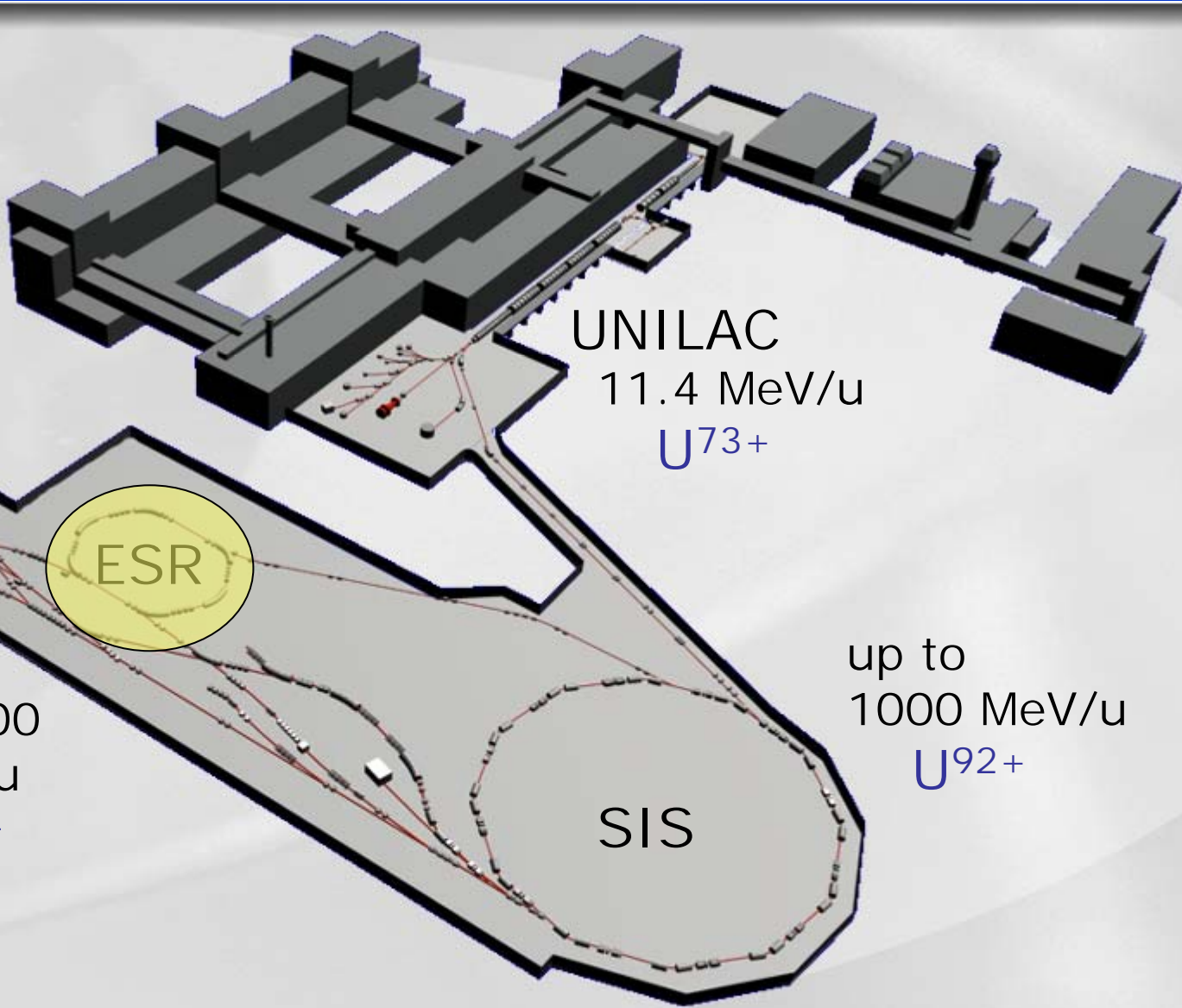
1994: U. Müller-Hehler and G. Soff, **Electron excitations in superheavy quasimolecules** Phys. Reports **246**, 101.



HCI Production at GSI-ACCELERATOR FACILITY



Internal Gas-jet Target



First Step in ESR Studies of K-Shell Excitation and Ionization at Small Impact Parameters and in Symmetric Heavy Systems

Overall Goals

Extend ESR studies to new regimes, e.g., to study

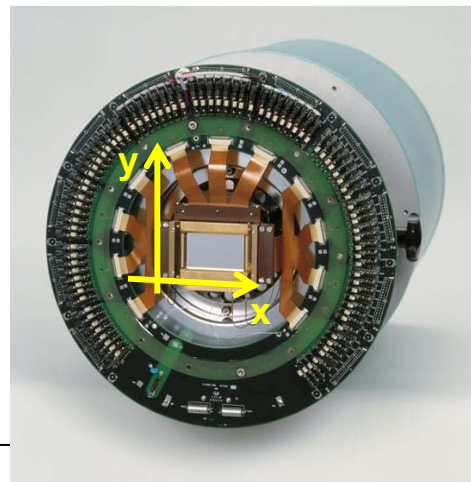
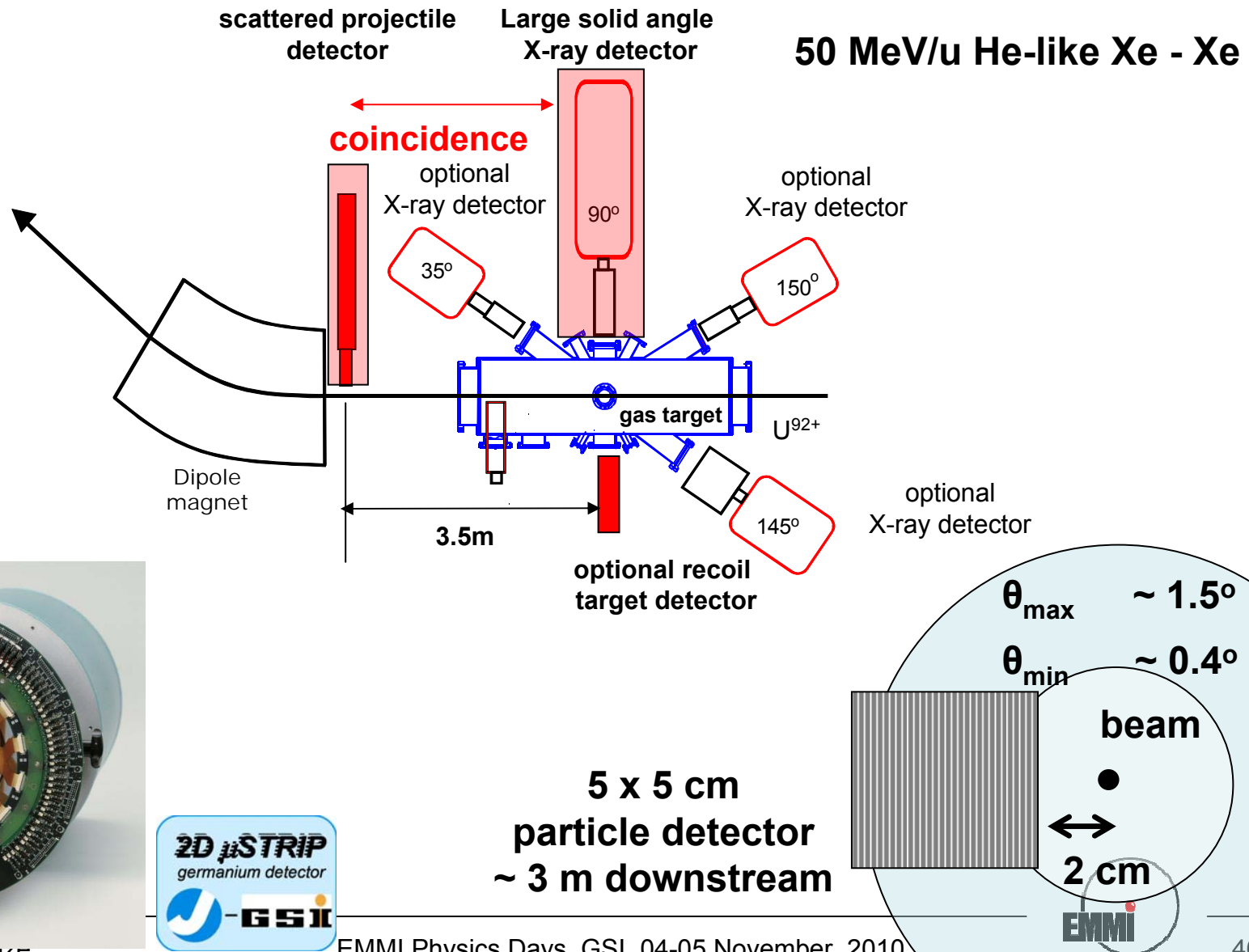
- symmetric heavy particle interactions where the combined nuclear charge is >100
- K-shell excitation and ionization processes at small impact parameters (much less than K-shell radius, e.g. < 200 fm)
- excitation and ionization of quasi-molecules produced in slow collisions

First Step

- Measure K-shell excitation at small impact parameters for "symmetric" heavy particle system, e.g., **50 MeV/u He-like Xe- Xe or 100 MeV/u He-like Au - Xe.**
- Investigate signal rates and backgrounds and use present study as a stepping stone for future impact parameter studies of K-shell ionization, excitation, and radiative electron capture.
- Test possibility of using the ESR and internal gas target to measure MO radiation produced in very heavy quasi-molecules.



Proposed Study: Experimental Method

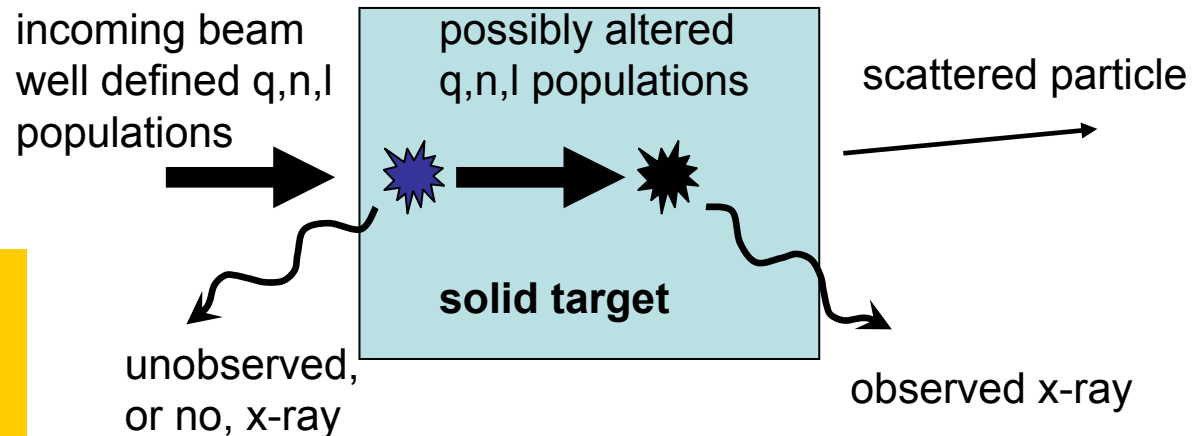


Advantages and improvements as compared to the previous studies

- incoming ion in a well defined and desirable charge-state
- gas-target: single collision conditions
- outgoing ion charge-state undisturbed

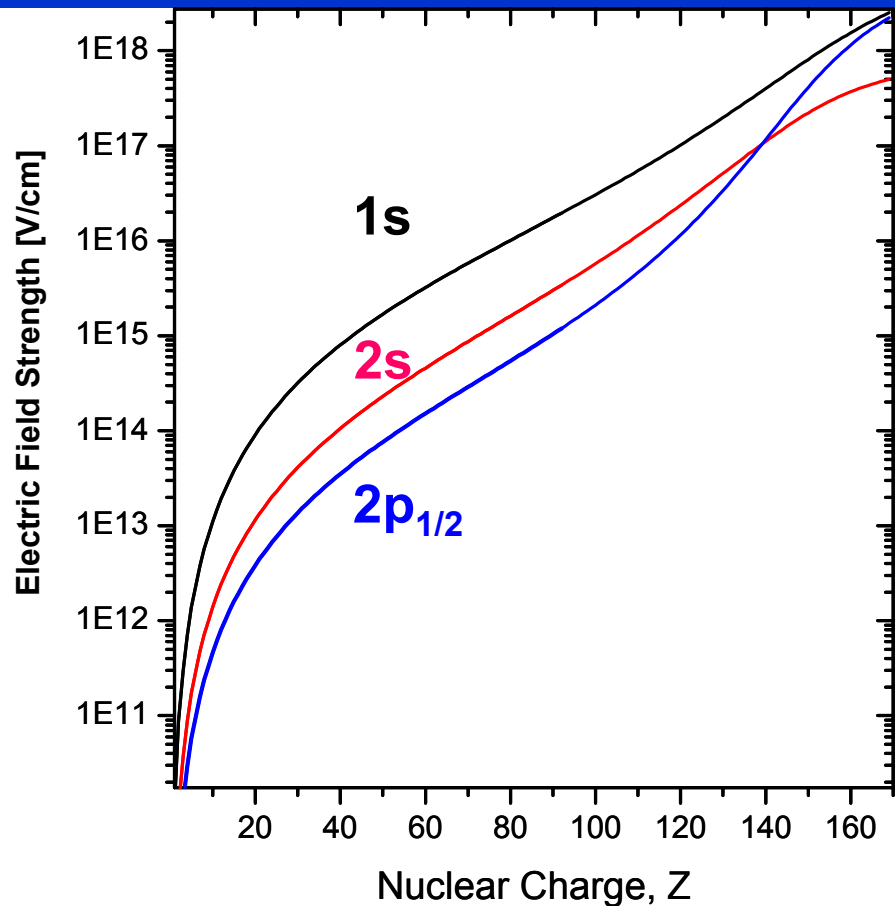
Advantage:
high signal rates,
very high Z_{targ} possible

Dissadvantage:
data must account for
possible alterations in initial
and final q, n, l populations.



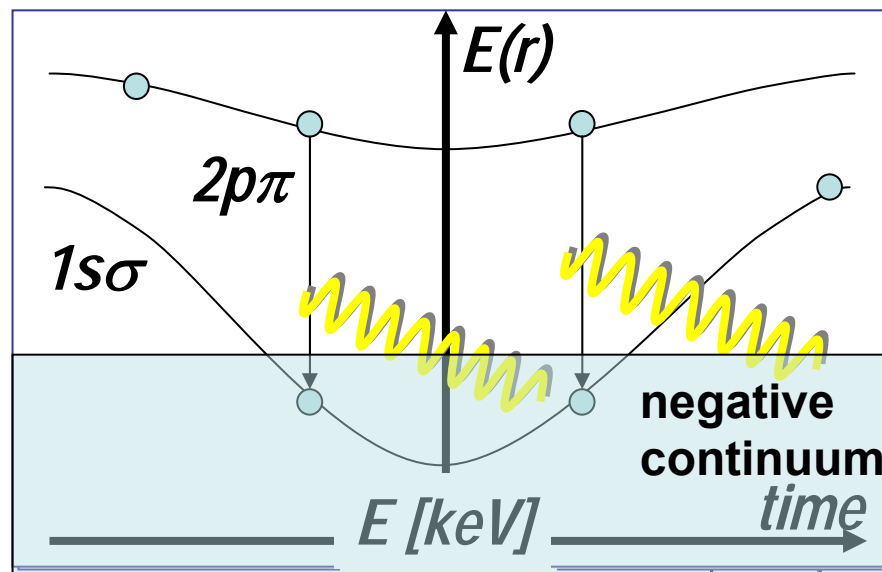
- possibility to conduct experiments in a wide collision energy range
(Deceleration capability of the ESR)
- novel segmented solid-state detectors: position, energy and time resolution

Critical- and Super-Critical Fields

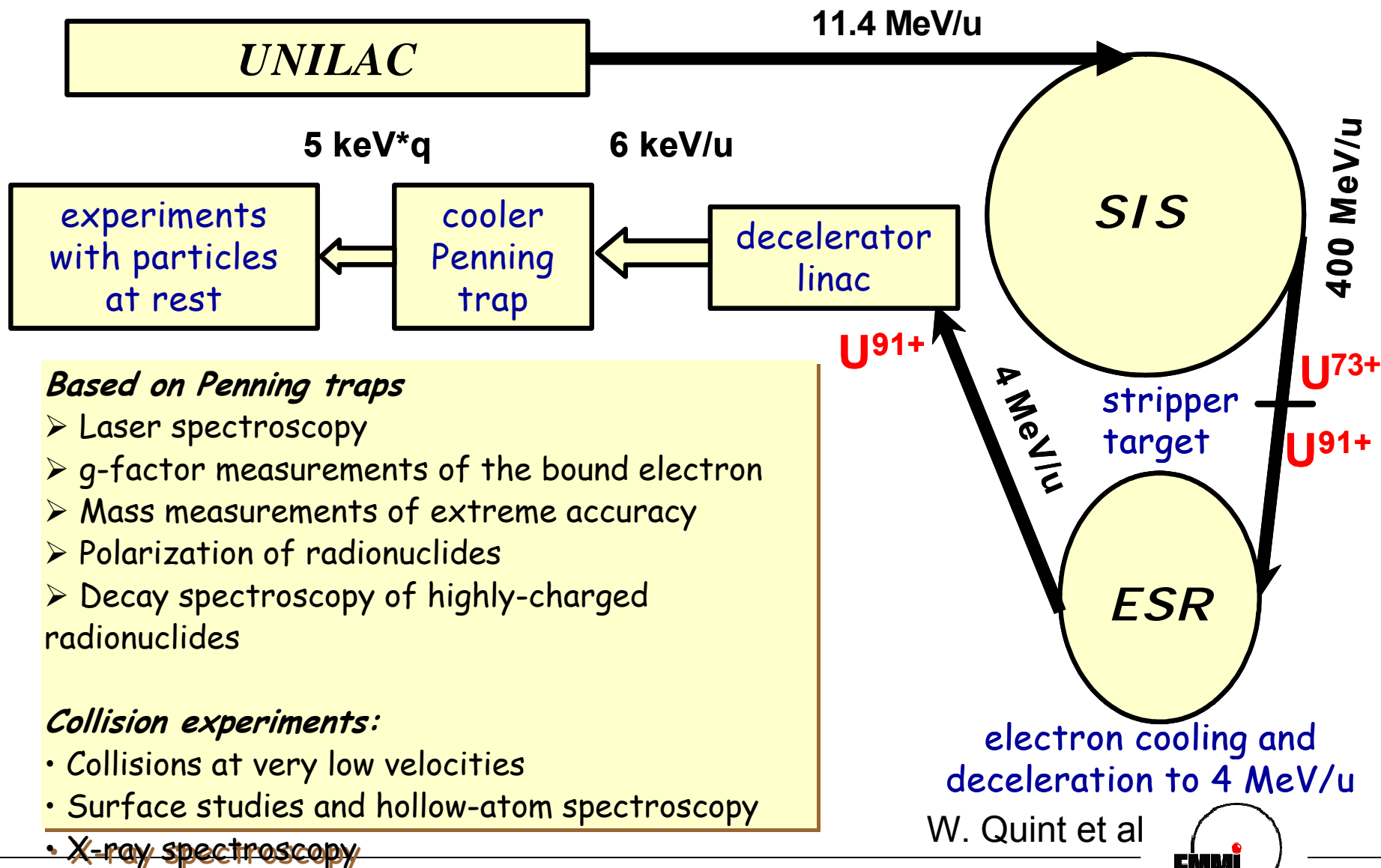


spectroscopy of the inner shells in superheavy quasimolecule systems with energy eigenvalues in the vicinity of the negative continuum

$U^{92+} \rightarrow U \Rightarrow$
 $U^{91+} + MO-X-Ray \dots$



HITRAP overview



Summary

Precision Studies of Atomic Structure at High-Z

- $1s$ LS in H-like uranium confirmed on a level of 1%
- Further progress towards an absolute accuracy of 1 eV is expected from high-resolution spectroscopy techniques (Beamtime beginning of next year)

Atomic Collision Dynamics and Photon-matter Interaction in Strong Perturbative Regime

First experimental studies of excitation for the Heaviest H-like Ion in Relativistic Collisions

Exploiting Atomic Physics techniques for Exploring Plasmas Generated by High-power Laser

Hot electron energy distribution

Various precision experimental tools developed and available in fundamental atomic physics research with heavy ions can be successfully utilized for exploring extreme states of matter.



Outlook

Atomic Physics at Extreme Fields at GSI Darmstadt and at the FAIR Facility

Critical- and Super-Critical Fields

spectroscopy of the inner shells in superheavy quasimolecule systems with energy eigenvalues in the vicinity of the negative continuum

Outlined a new experimental ESR program based upon a new observable, the impact parameter. This will allow us to study K-shell ionization, excitation, and radiative electron capture in more detail than previously possible.

Described an upcoming experiment which will establish techniques, signal rates, and backgrounds for planning future studies.



Collaboration

EMMI / GSI

D. Banas, H.F. Beyer, G. Bednarz, F. Bosch, W. Chen, S. Hagmann, S. Hess
O. Klepper, C. Kozhuharov, D. Liesen, P.H. Mokler, X. Ma, R. Märtin, R. Reuschl, U. Spillmann
M. Steck, Z. Stachura, Th. Stöhlker, S. Tashenov, D. Thorn, S. Toleikis, S. Trotsenko, A. Warczak,
G. Weber, D. Winters, N. Winters,....

HYI Group, Univeristy of Frankfurt

R. Grisenti, N. Petridis,....

Laboratoire Kastler Brossel (LKB), Paris

P. Indelicato, C.I. Szabo

Missouri University of Science and Technology, Rolla, USA

R.D. DuBois

Theory

A. Surzhykov, S. Fritzsche, A. Artemyev, V. Shabaev

